AD NUMBER

AD482633

LIMITATION CHANGES

TO:

Approved for public release; distribution is unlimited.

FROM:

**Distribution authorized to U.S. Gov't. agencies and their contractors;
Administrative/Operational Use; APR 1966. Other requests shall be referred to Air Force Materials Lab., Wright-Patterson AFB, OH 45433.**

AUTHORITY

AFML ltr 24 Apr 1970

AFML-TR-65-375
VOLUME I

THERMAL CONTACT RESISTANCE

VOLUME I — A REVIEW OF THE LITERATURE

MERRILL L. MINGES

TECHNICAL REPORT AFML-TR-65-375, VOLUME I

APRIL 1966

AIR FORCE MATERIALS LABORATORY
RESEARCH AND TECHNOLOGY DIVISION
AIR FORCE SYSTEMS COMMAND
WRIGHT-PATTERSON AIR FORCE BASE, OHIO

NOTICES

When Government drawings, specifications, or other data are used for any purpose other than in connection with a definitely related Government procurement operation, the United States Government thereby incurs no responsibility nor any obligation whatsoever; and the fact that the Government may have formulated, furnished, or in any way supplied the said drawings, specifications, or other data, is not to be regarded by implication or otherwise as in any manner licensing the holder or any other person or corporation, or conveying any rights or permission to manufacture, use, or sell any patented invention that may in any way be related thereto.

Copies of this report should not be returned to the Research and Technology Division unless return is required by security considerations, contractual obligations, or notice on a specific document.

200 - May 1966 - 773-42-915

AFML-TR-65-375
VOLUME I

THERMAL CONTACT RESISTANCE

VOLUME I — A REVIEW OF THE LITERATURE

MERRILL L. MINGES

AFML-TR-65-375
Volume I

FOREWORD

This report was prepared under Task 7381, "Materials Applications", Project 738106, "Design Information Development" with Merrill L. Minges acting as the project engineer. The work was carried out over the period from 1 January 1964 to 1 May 1965.

This report is the first volume of a three volume series dealing with the theory, measurement and interpretation of interfacial heat transfer effects as they apply to high temperature components of advanced weapons systems. The second volume, to be issued shortly, is entitled "Thermal Contact Resistance: An Apparatus for High Temperature Measurements". The third volume which is now in preparation will be entitled "Thermal Contact Resistance: Temperature Dependency".

Manuscript released by the author December 1965 for publication as an RTD Technical Report.

This technical report has been reviewed and approved.

W. P. CONRARDY, Chief
Materials Engineering Branch
Materials Applications Division
Air Force Materials Laboratory

ABSTRACT

The objective of this report has been to critically review the status of experimental and analytical developments in the area of heat transfer across interfaces of solids in contact. The nature of the heat flow patterns which develop across an imperfect interface are first discussed along with the equations defining the thermal contact resistance parameter. Following this a general discussion is given of the practical application areas where interface heat transfer is an important design parameter. The next sections of the report give a thorough presentation of the analytical analyses which have been developed to describe this phenomena. Surface deformation effects, geometrical characterization of surfaces and the influences of void phase conduction are outlined. Correlations of experimental results with analytical predictions are covered in the final section using the equations derived for the single and multiple contact cases. Some of these correlations are based on limited experimental data, others are more generalized in nature.

CONTENTS

ILLUSTRATIONS

TABLES

SYMBOLS

A	= stream tube cross-section
a	= contact radius
b	= "feeder element" radius for single contact
C	= constriction number
D	= indenter diameter
d	= indentation diameter
E	= modulus of elasticity
f	= constriction alleviation factor
g	= accommodation coefficient jump distance
H	= hardness
h_c	= thermal contact conductance
J_o	= Bessel function
K	= dimensionless conductivity number
k	= thermal conductivity
L	= load
ℓ	= equivalent length
M,m	= empirical constants
N_{Pr}	= Prandtl number
q	= heat flux
R_c	= thermal contact resistance
r, z	= cylindrical co-ordinates
S_1, S_2, S_3	= surface profile characterization parameters
T	= temperature
U	= dimensionless conductance number
u	= degree of flattening

SYMBOLS (Cont'd)

X	= constriction ratio
Y	= elastic limit
α	= constant
γ	= specific heat ratio
δ	= effective gap width
$\frac{\partial}{\partial n}$	= normal differential
ϵ	= strain
λ	= mean free path
μ	= Poisson's ratio
ξ	= deformation factor
ρ	= electrical resistivity
σ	= standard deviation
ψ	= potential function

SECTION I

INTRODUCTION

When two surfaces are brought together to form an interface the true solid-to-solid contact area between them is generally a small fraction of the apparent area over which they meet. This direct contact area may be less than 1 percent of the total and rarely exceeds 10 percent unless bonding agents are introduced. This characteristic of interfaces has great practical significance in the understanding of frictional properties of surfaces and in the transfer of electrical and thermal energy across contiguous surfaces.

In the case of energy transfer when a uniform gradient is applied axially along adjoining members which have a common interface, as shown in Figure 1a, the net effect of the interface on the transport process is the formation of a temperature or voltage discontinuity as shown. This discontinuity results from the imperfect nature of the contact as drawn schematically in Figure 1b. As the interface is approached the flux lines tend to converge to the direct solid-to-solid contact points since for metallic contacts this flow path offers considerably less resistance than the void areas around the contacts which are generally filled with air or may be evacuated. If the contact members have low conductivity, comparable to that of the void volume component, the distribution would be altered. This convergence of the flux lines to the solid-to-solid contact areas produces a "constriction resistance" and an interfacial potential drop to compensate for it. This is demonstrated in Figure 1b where the equipotential surfaces (1) and (2) which are orthogonal to the flux field are seen to curve away from the contact plane at the constriction points. In the heat transfer case this implies that, on the average, the isotherm (1) is at a higher temperature than it would be in the absence of an interface and that the isotherm (2) is at a lower average temperature. The net effect then is the formation of a temperature discontinuity at the interface as shown in Figure 1a.

Quantitatively, this interfacial resistance to energy transport is expressed as the ratio of the potential drop encountered at the interface divided by the flux crossing the interface. For the heat transfer case the defining equation for the thermal contact resistance R_c is as follows,

$$R_c = \frac{1}{h_c} = \left(\frac{\Delta T}{q}\right)_{interface} \qquad (1)$$

where,

R_c = thermal contact resistance, hr-ft^2-^{o}F/BTU

h_c = thermal contact conductance, BTU/hr-ft^2-^{o}F

ΔT = interfacial temperature drop, ^{o}F

q = interfacial heat flux, BTU/hr-ft^2

It is clear that this contact resistance is a function of the physical and chemical characteristics of the contacting surfaces (for example, rough, wavy, oxidized, plated), the compressive force with which they are held together, the ambient environment, and temperature level. These factors will be considered in detail later, however, several factors of general importance can be mentioned here.

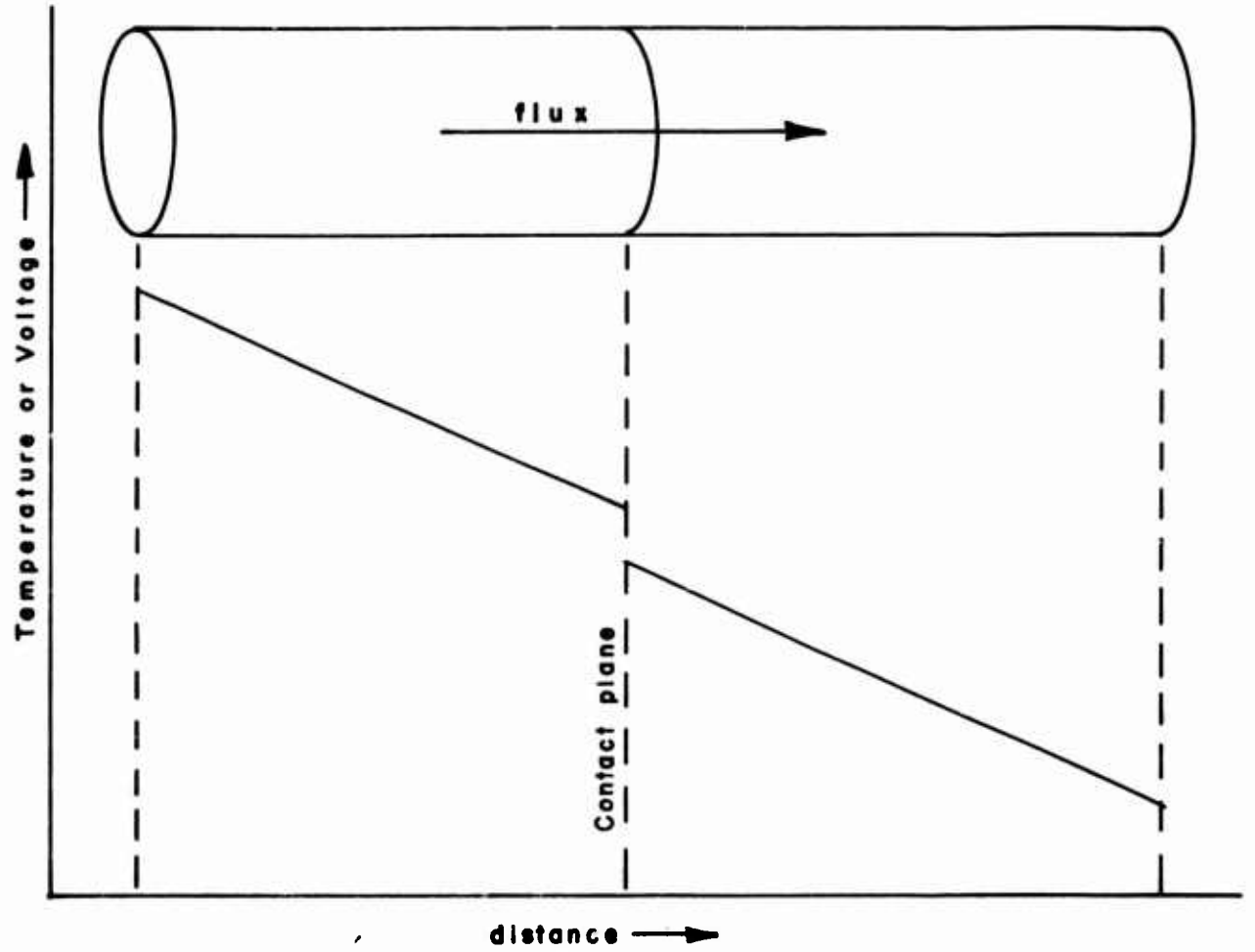

Figure 1a. Interfacial Resistance Reflected as Potential Discontinuity

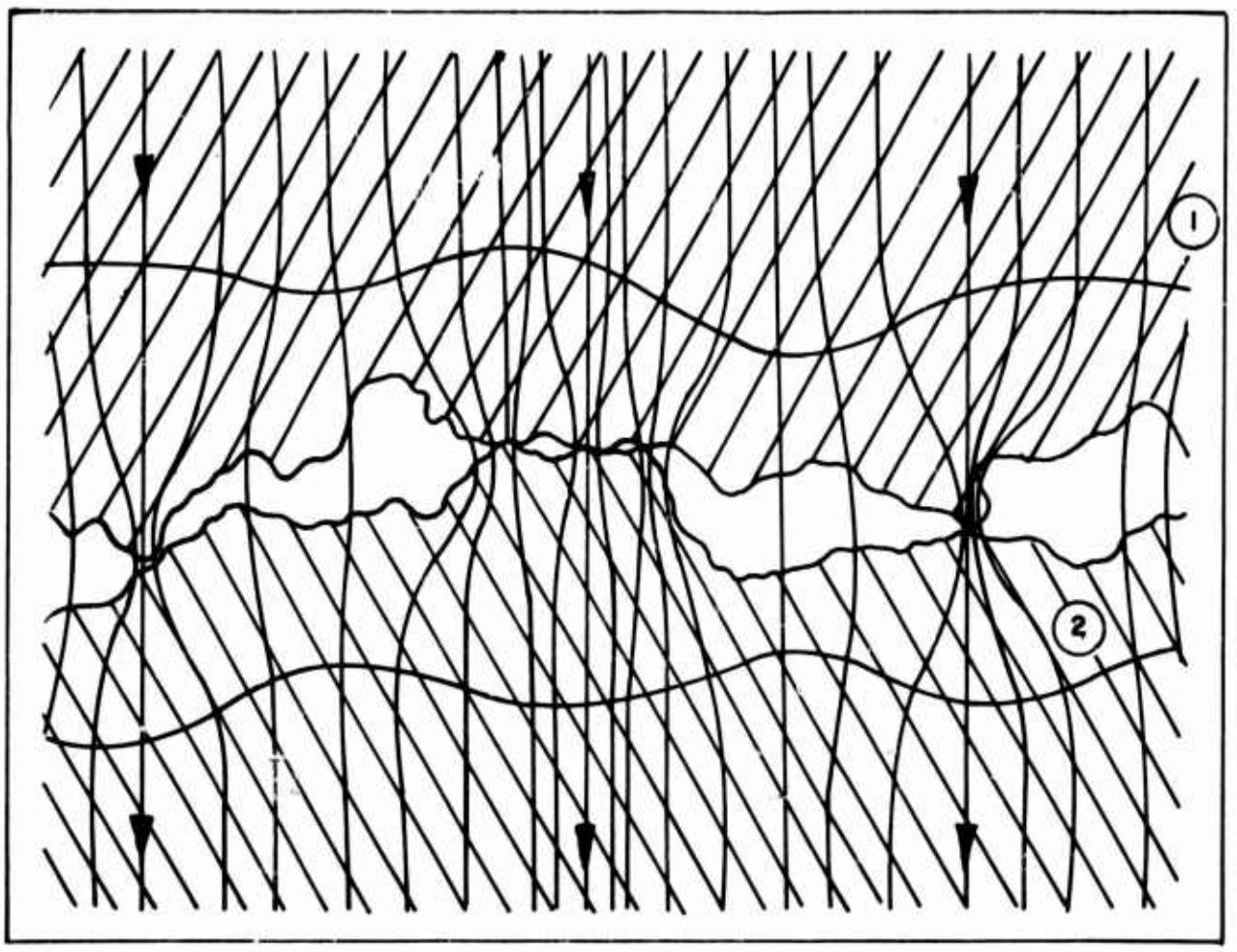

Figure 1b. Flux Field Distribution at an Interface

Most analytical formulations of contact resistance equations begin by considering the heat flow through a single idealized contact. The analyses are then expanded to cover more practical interfaces which are made up of a number of contacts. As will be derived later on, the contact or constriction resistance for a single contact point resulting from the flux line convergence depicted in Figure 1b is given in Equation 2 where the contact radius is a.

$$(R_c)_{\text{one contact}} = \frac{1}{2ka} \qquad (2)$$

k = thermal conductivity, BTU/hr-ft-^{o}F

a = contact radius, ft

The simplicity of Equation 2 belies the nature of the subtle problems encountered in extending the result to practical multiple-contact interfaces. To do this, mechanical deformation characteristics of the surface asperities must be known since compressive loading is an important parameter. These are difficult to estimate since both plastic deformation of the asperities and elastic stress field formation in sublayers occur. These in turn are complicated by work hardening and creep effects. Surface contamination from oxide films or various impurities may be very important for two reasons. First, such layers generally have low conducitivity relative to the contact members. Second, these film resistances are contact area dependent whereas the constriction resistance, Equation 2, is linear in contact dimension or proportional to the square root of the contact area. Heat transport across the void areas may occur by gas phase conduction and radiation. These are dependent both on the geometry of the void areas which is complex and on the temperature level. Temperature variations in turn may influence mechanical deformation characteristics.

In studying any of these factors it is necessary to have complete and accurate information on the geometry of the surfaces making up the contact. Inattention to the definition of surface characteristics has greatly limited the utility of a large volume of carefully measured contact resistance data. Of particular importance has been a lack of complete data on the different degrees of roughness encountered with most practical surfaces. Not only is microscopic roughness resulting from conventional forming and finishing operations present but also roughness on a larger scale which could be manifested as surface waviness of various degrees or in the extreme as surface curvature. The influence on the constriction resistance of these different types of surface irregularities, which may span several dimensional orders of magnitude, is clearly shown in Figure 2. Here for several values of the total solid-solid contact area the contact conductance or the reciprocal of the constriction resistance has been plotted as a function of the number of contact points making up this total contact area. For a given total solid-solid contact area, the contact conductance increases greatly as the number of contact points making up this area increases. Thus, if an interface happens to be made up of surfaces that are both rough and wavy, which is highly likely in most cases, relatively large contact regions governed by the waviness will be formed. Each of these areas will consist of a number of smaller solid-to-solid contact points, the size and distribution of which is governed by the surface roughness. From Figure 2 it is clear that the overall constriction resistance of the interface may be governed by the surface waviness and not the roughness.

These considerations should be sufficient to indicate that energy transport across interfaces is a complex phenomena when practical types of interfaces are involved. Resistance effects in electrical contacts has been a problem receiving

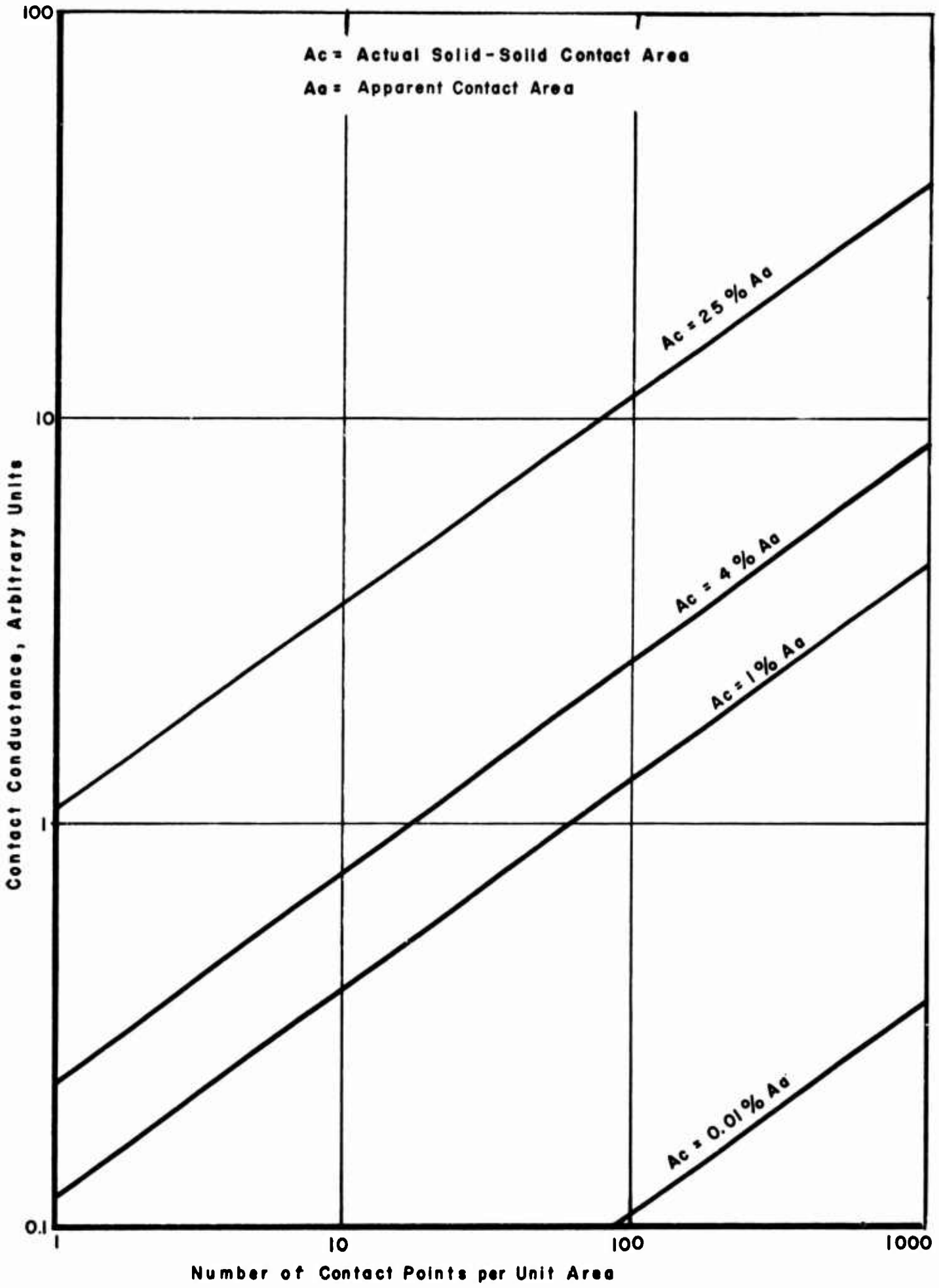

Figure 2. Effects of Constriction on Contact Conductance (Reference 1)

attention for many years. Recently the electrical resistance of interfaces in thermoelectric power devices has been studied extensively since this factor greatly limits their efficiency. It is only in the last few years that the area of thermal contact resistance has become of real practical importance. The following list summarizes areas where such information is required in engineering design:

A. AIRCRAFT STRUCTURES

Operation at hypersonic speeds induces substantial heating of structural joints. Estimation of temperature distributions and in turn thermal stresses requires a knowledge of the contact conductance between structural components.

B. PROPULSION SYSTEM DESIGN

For high efficiency in both turbine powered engines and in solid and liquid fueled rockets operation at very high temperatures is desirable. Heat dissipation from turbine blades and through the composite liners of rocket nozzles and exit cones is across mechanical interfaces which may be metallic, graphitic, ceramic or combinations thereof. Contact conductance information is required in these applications for both thermal and mechanical design.

C. SPACE VEHICLE SYSTEMS

Carefully controlled dissipation of heat from electrical power, guidance and communication modules is required to maintain operating temperatures within narrow limits. Similar control is also necessary in crew areas. Interfacial heat transfer under vacuum conditions is an important design parameter in these applications.

D. NUCLEAR REACTOR OPERATION

Conventional fuel elements for reactor applications are constructed with a cladding or sheath usually of a low neutron absorption alloy. Since very high heat fluxes cross the interface between the fuel and cladding even moderate contact resistance can lead to large, undesirable temperature drops. Since the fuel often consists of a relatively brittle enriched oxide the contact resistance tends to be substantial.

E. THERMAL MEASUREMENT EQUIPMENT

In measurements of thermal transport properties of liquids, solids and composites and in general instrumentation for temperature measurement, precautions are always taken to minimize temperature discontinuities. Since temperature sensing elements are most often located in metered heat flux areas both perturbation of the flux field and temperature reading errors are dependent at least partially on interface resistances. If the arrangement is such that analytical corrections can be made for interface effects, data on contact resistance coefficients must be available.

In the section that follows dealing with applications, the literature on contact resistance covering the above areas will be reviewed in some detail. With this background the remaining sections of the review will be concerned with analytical analyses and development of quantitative relationships for thermal contact resistance and their use in correlating experimental data. As indicated earlier the most logical starting point in the analytical development is with the single contact case. It is covered in Section III. In Section IV the results are expanded to cover the complex but practically important cases of multiple contact interfaces.

Finally, in Section V a brief review is made of studies where successful correlations of experimental results and analytical predictions have been effected on multiple contact interfaces. These predictions are based on interface contact models with varying degrees of refinement. In many instances, highly empirical analyses are used, and thus successful experimental data correlation did not necessarily represent a full understanding of the heat transfer processes involved. This last section, which is based on the principles discussed in earlier sections, is intended to give a fairly clear indication of the present state of affairs in understanding the complex thermal-mechanical phenomena which collectively compromise interfacial contact resistance.

SECTION II

ENGINEERING APPLICATIONS

Several of the areas where thermal contact resistance is an important design parameter have been mentioned previously. In this section the role of interfacial heat transfer in such applications will be summarized. Consideration will be limited to those instances where heat transfer occurs across solid-solid interfaces since heat transfer across solid-liquid and solid-gaseous interfaces are physically different processes and are handled in a different manner analytically. Solid-solid interfaces are developed which consist of metallic, ceramic, graphitic or intermetallic members as well as various combinations thereof. In addition, composite interfaces are encountered where soft shim materials in the form of foils or as plating are used to reduce interfacial resistance; grease coatings have also been used where their application is practical.

To give an idea of the magnitude of interfacial resistances encountered in engineering practice, Table I has been prepared. Values can vary greatly with surface finish, compressive loading, temperature, and so forth. The values in the Table are typical, however, of nominal surface finishes (20 to 200 μ in. RMS) at compressive loading levels common in bolted or riveted structures (up to several hundred psi) around room temperature. Besides the direct use of interfacial heat transfer coefficients in heat transfer design, it is common to express interface resistance values in terms of the equivalent thickness of a given material required to generate the same temperature drop as that produced by the interface. In some cases an "equivalent air gap" is used; in Table I the equivalent thickness of stainless steel was calculated since this is a more meaningful measure of the resistance effect of an interface on structural temperature distributions. From the definition

TABLE I

RANGES OF THERMAL CONTACT CONDUCTANCES UNDER MODERATE LOADS

Interface	h_c, BTU/hr-ft^2-^{o}F	Equivalent Thickness Inches of SS: (k=175 BTU-in/hr-ft^2-^{o}F)	Literature Reference
Ceramic/Ceramic	100 - 500	0.3 - 1.7	2
Ceramic/Metal	250 - 1500	0.1 - 0.7	2, 3
Graphite/Metal	500 - 1000	0.1 - 0.3	2, 4
Steel/Steel	300 - 1500	0.1 - 0.7	4, 5, 6
Aluminum/Aluminum	500 - 5000	0.03 - 0.3	2, 6
Metal/Metal (Joint Filler: Soft Metal Foil or Grease)	5000 - 15,000	0.01 - 0.03	2, 7

of h_c, Equation 1, the equivalent thickness is clearly the ratio between the stainless steel conductivity and the contact conductance value, h_c. Contact conductance values can range over more than two orders of magnitude for different types of interfaces under moderate load conditions. Increases on this same order may occur for a given interface when the compressive load is increased to several thousand psi.

A. AIRCRAFT STRUCTURES

Temperature effects on structural stress distributions and mechanical strength become significant only for high speed flight. They become of concern in supersonic aircraft design and may be critical for sustained hypersonic flight or atmospheric re-entry when very high temperature - high heat flux conditions occur.

Most of the experimental studies in this area have relied on highly empirical correlations. Small sections of bolted, welded or riveted structural components have been exposed to both steady state and transient heating while joint temperatures discontinuities are being observed (References 8, 9, 10, and 11).

Early work at Syracuse University by Barzelay and co-workers under NASA sponsorship first attacked the problem of thermal resistances in aircraft structural joints by conducting a large number of steady-state measurements using simple disk specimens of aluminum allow and stainless steel aircraft alloys (References 12, 13). Bare metal-metal contacts were studied along with contacts separated by thin foils of brass, insulating sheets of asbestos, and adhesively bonded interfaces. Interface conductance values ranging from about 100 to 4000 BTU/hr-ft^2-^{o}F were observed; the high conductivity shim materials improved the conductance significantly. This work was later extended to measurements on riveted skin-stringer combinations under transient heating conditions. It was found that the range of normal conductances for those aluminum and steel alloy simulated structural components was somewhat lower than that of the simple disk specimen combinations because flatness control was more difficult, (References 14, 15). Similar tests were conducted with riveted skin-stringer combinations of high temperature Inconel and titanium alloys (Reference 16). Analysis of the transient heating results indicated that the riveted interfaces had significant effects on the temperature distributions on all geometries tested and therefore on the stress distribution calculations. It was found that the interface conductance values depended both on heating rate and local temperature drop. This effect was associated with warpage of the components during heating. A similar dependence of normal stresses induced by contact resistance on heat input and geometry was observed by Gatewood (Reference 17).

Variations in rivet size, pitch and placement were found to cause variations in the average interface heat transfer coefficient. This effect is caused by the fact that the compressive load on the joint varies with different rivet geometries while the overall load distribution along the joint changes with rivet placement. On the average a 30 percent variation in load was observed between the rivet area and point midway between the rivets.

Instead of measuring overall joint conductance values for riveted structures which averages out load variations along the joints a more refined approach would be to calculate the compressive load distributions around various rivet configurations and then apply contact conductance data as a function of load for simple interfaces in an area integration to obtain the average joint conductance. This approach has been studied by Lardner (References 18, and 19). After the form of the midplane stress distribution around a bolted joint with cylindrical symmetry had been

established the effect of variable joint conductance on the axial temperature discontinuity was calculated. With data available on the functional relationship between contact conductance and load, the spatial variation in interface conductance was immediately established from the load distribution. For a linear radial variation in the contact conductance it was found that the average interfacial temperature drop was higher than for the case where the conductance was assumed constant. A similar approach was used by Aron and Colombo (Reference 20) in studying the radial variation in contact conductance around bolted joints simulating those between spacecraft electronic components and heat sinks.

Detailed studies of joint conductance effects on the performance of rather complex skin-stiffener panels were conducted by Griffith, et. al (References 21, and 22). The test sections consisted of two skin members separated by a stiffener and heated on their outer surfaces. As observed elsewhere, the joints greatly alter temperature distributions and increase thermal stresses. Internal radiation tended to smooth the temperature distributions and thus reduce stresses. At higher temperatures these two effects tended to cancel one another. In a Mach 2 jet tunnel test of a multiweb wing section, flutter and dynamic failure resulting from poor thermal contact in the riveted joint was observed.

In cases where it is possible to define an average contact resistance parameter independent of localized stress distributions, generalized design curves with contact resistance as an explicit parameter have been worked out to predict the effects of joint discontinuities on temperature and stress distributions. This approach has been pursued by Pohle, et. al (Reference 23) and Barber, et. al. (Reference 24). The use of such generalized approaches depends on the availability of accurate interface resistance data which covers a substantial range of materials, surface condition and loads. The fact that highly empirical testing of practical structural joints has been the accepted engineering practice in estimating contact conductances rather than more general but highly refined analysis based on load distributions reflects the complexities encountered in the latter.

B. PROPULSION APPLICATIONS

Both turbine and rocket nozzle applications are characterized by high temperatures, reactive environments, and thermal transients produced under high heat flux conditions. Estimating intercomponent heat transfer is a difficult design problem since the geometry of high temperature sections of jet propulsion units are obviously quite complex; the same may be true in ablative and regeneratively cooled rocket nozzle throats and extensions.

As in reactor fuel element applications analyses of interface conductance effects in rocket nozzles are complicated by the presence of cylindrical contact surfaces and by substantial thermal expansion differentials between adjacent layers produced as a result of wide temperature variations under operation. The idea of using refractory metal liners directly in contact with the gas stream in liquid rocket engines to produce an insulating thermal resistance layer to inhibit radial heat flow has been studied by Hines (Reference 25). If the contact resistance were controlled within a rather wide interval it was indicated that the liner could be used to replace or supplement regenerative cooling. This approach is then a useful application of a resistance effect which has been troublesome in liquid rocket engines - the formation of a high thermal impedance coating or deposit which reduces the cooled chamber wall temperature and increases the temperature of the internal nozzle surface (Reference 26). Hines concluded that contact conductance values between the

liner and nozzle sublayers in the range from 500 to 7000 BTU/hr-ft^2-^{o}F were required to produce effective liners at rocket nozzle heat flux levels up to 18 BTU/in^2 - sec. The required conductances are within the range shown in Table I. Depending on specific operating conditions the allowable interface conductance values may fall in a narrow interval. If the interface conductance were too low, the liner temperature could increase beyond the limit of the refractory metal since gas temperatures are often 5000^{o}F or higher. If the conductance were too high, the liner would not be effective. The results of simple tests with a cylindrical liner-heater arrangement indicated that the approach was at least qualitatively feasible. It was also concluded that, for a rigidly contained system, differential thermal expansion had the greatest effect on h_c.

In turbine applications the maximum flux levels are considerably below those of liquid rockets, ranging from 0.1 to 1.0 BTU/in^2 - sec. Russian authors have done a considerable amount of work on contact conductance effects on these turbine propulsion systems (References 27, 28, and 29). This activity concerning heat transfer between contacting surfaces of different metals was initiated in 1953 at the Institute of Power Engineering of the Academy of Sciences of the UkSSR. A listing of a large number of papers on the subject published by the Institute are included in Reference 27. It was found that interfacial temperature drops between turbine components could range up to 100^{o}F at the higher flux levels. Differential thermal expansion under these conditions could have a detrimental effect on press-fit joints through relaxation of the compressive load. Experimental investigations of interface heat transfer coefficients were carried out with specimens forming planar interfaces representative of different groups of turbine construction materials. Several steels, copper, brass aluminum alloys were tested having surface finishes in classes 7 to 9 (20 to 200 μ in.).

Experimental and analytical studies with finned tubing components having joints similar to those of turbine components were made by Gardner and Carnavos (Reference 30). Fins of aluminum or copper were interference fitted in grooved stainless steel tubing. The condition of complete loss of intermetallic contact as a result of thermal relaxation of the contact pressure was investigated with the formulation of equations for predicting initial contact pressures and the variation in gap resistance as a function of temperature. Experimental substantiation of the results was fair.

For high efficiency and greater thrust levels operating temperatures in turbines are increasing as are the pressures and temperatures in rocket engines. Because of the multiple starts these power units encounter in use, it is difficult to estimate intercomponent loading which arises from differential expansions; temperature induced plastic deformation and creep are complicating factors. The geometries encountered are complex too so that contact conductance studies in the area have generally been limited to establishing the ranges of values likely to be encountered across interfaces of typical turbine and rocket construction materials. Planar interfaces are usually studied under variable compressive loading.

C. SPACECRAFT APPLICATIONS

Only recently has any great emphasis been placed on the measurement of contact resistance under vacuum conditions. Heat transfer calculations in space vehicle systems have lead to requirements for this type of information. Several general studies in the area have been sponsored recently by NASA (References 31, 32, and 33). Similar studies have been NASA sponsored dealing specifically with the Saturn system

(References 34, and 35). Other work under vacuum conditions covering the cryogenic temperature range has been completed on spacecraft alloys by Bloom (Reference 37), and for the Apollo project by Jannson (Reference 36). In most instances the objective has been a reduction in the contact resistance to as low a level as practical. It has been generally observed that vacuum environment contact resistances are high compared with values for the same interfaces in air due to the absence of gas conduction contributions. However, since the interfaces operate at relatively low temperatures in most spacecraft systems a variety of low vapor pressure greases and thin foils of soft metals such as lead, indium and gold could be used to decrease the contact resistance.

Tests at very low interface loads (5 to 35 psi) in vacuum with large, flat aluminum alloy specimens conducted by Fried (Reference 38) showed that lead and aluminum foils decreased the contact resistance by a factor of 2 or 3. A silicone grease was found to yield about the same reduction in contact resistance. As would be expected, the grease was effective even at loads of about 2 psi (Reference 39). A similar investigation by Cunnington (Reference 7) with magnesium and aluminum alloys in the load range from 5 to 100 psi showed that silicone grease increased the interface conductance by a factor of 10 (from about 100 to 1000 BTU/hr-ft^2-^{o}F). One mil indium foil as the filler material increased the conductance another factor of 10 to around 10,000. Values above 10,000 were measured on aluminum and beryllium interfaces with indium foil fillers in the Apollo project studies (Reference 36).

In the Saturn IB/V vehicle most of the electronic equipment units are mounted directly to liquid cooled heat sink panels. Since operation is under space environment conditions all heat will be dissipated by solid conduction across the interface between the component housing and the cold plate. These interfaces of dissimilar light metals were designed with contact pressures of about 1000 psi. Experimental measurements on the magnesium and aluminum alloys used in the vehicle indicated that the interface conductance values were high enough to cause interface temperature differentials of only about 2^{o}F (References 34, and 35). Heat loads in these applications are low, however, averaging around 1200 BTU/hr-ft^2.

Further tests with practical spacecraft interfaces and components at low interface loads were carried out by Petri (Reference 41) and Stubstad (Reference 40). Of the 20 different filler materials considered by Stubstad indium foil was rated among the best. It was suggested that interfaces formed in air at atmospheric pressure and then tested in vacuum would not reach the same condition as the vacuum environment thus complicating analysis of the experimental results. Results of another experimental study on the gas leak through metallic contacts showed that in the molecular flow regime the conductance of the interface for lateral gas flow was proportional to the square of the surface roughness (Reference 42). If waviness were significant the gas conductance would be substantially greater. For extremely smooth surfaces the waviness can be substantial, thus unless soft fillers are used or the initial compressive loads are very high, the interface voids should rapidly reach the same gas pressure levels as the surroundings.

Employment of cryogenic fluids as power sources for space vehicles has been found to be practical because long term storage is facilitated by the use of reflective foil composite thermal insulations. These insulations are highly efficient when vented to the hard vacuum of space. Serious design problems can occur, however, as a result of heat shorts from structural support members and piping. The same problem is encountered in ground hold and transport of cryogenic fluids. As a possible solution to the problem of designing structural supports which are of low conductivity Mikesell and Scott (Reference 43) have proposed the use of a layered arrangement of

thin metallic disks. The insulating effect of the composite is derived from the series arrangement of the contact resistances between the disks. For 0.0008 inch stainless steel, heat conduction through the plates at a load of 100 psi was only 2 percent that of the metal. Thicker plates had a higher resistance per contact since deformation was less, however, the thin plates had a greater resistance per unit length of stack since the number of interfaces was greater. Similar tests with 0.002 inch stainless steel disks were conducted by Thomas and Probert (Reference 44).

For such cryogenic tankage applications particularly at the extremely low temperatures encountered with liquid or slush hydrogen (20°K) the temperature dependence of the contact conductance may be an important consideration. Berman (References 45, and 46) has found that this conductance is proportional to the square of the temperature level at helium temperature (4°K) for a variety of interface combinations. The dependence on temperature decreased as the temperature level increased. A similar temperature effect was observed by Little (Reference 47) where the heat flow was shown to be proportional to the difference of the fourth powers of the temperatures on each side of the interface. To date no systematic study has been made of the change in insulative efficiency of the disk composite with temperature in the cryogenic range.

In the design of complete satellite and spacecraft vehicles thermal scaling has been widely used. Subscale models have the obvious advantage of being readily accommodated in space simulation chambers of modest size. For thermal scale modeling in a high vacuum only conductive and radiative heat transfer occur. Based on these transport processes a series of eight basic dimensionless scaling groups can be defined (Reference 48). Under practical conditions Vickers has shown that only two scaling techniques should be considered (Reference 48), the technique of preserving temperature equality from model to spacecraft and the technique of preserving materials from model to spacecraft. In both cases one of the fundamental dimensionless groups is the contact conductance expressed in Biot modulus form. As a result of experimental studies on the applicability of scaling laws to simplified spacecraft models (Reference 49) it was concluded that extensive information was required on thermal contact conductance under vacuum conditions. In addition, practical methods of simulating interface conductances were found to be required since in some cases the scaling procedure required that the conductance ratio between model and spacecraft deviate from unity (e.g. identical materials case). A current effort under Air Force sponsorship is considering similar problems in radiative and interface heat transfer associated with the prediction of space vehicle thermal performance (Reference 50).

Finally, in the area of space power conversion a continuing problem has been efficient rejection of heat to the space environment via radiation. Effective heat dissipation implies large radiative areas while weight considerations, deployment and the protection of working fluid channels from meteoroid penetration impose serious practical constraints on radiator size. As a possible solution to these problems Rocketdyne has proposed the use of a moving belt radiator (Reference 51). This concept relies on the transfer of heat from the power system condensor, in the form of a rotating drum, to a moving belt which dissipates the heat to space.

The important design considerations in this concept are (1) materials compatibility, (2) interface conductance between belt and drum and (3) high temperature bearings all in the hard vacuum of space. The contact time between a given portion of the belt and the drum which operates around 1100°F is on the order of 250 milliseconds. It was established that the thermal diffusivity of the belt was high enough

that the efficiency of heat transfer was not limited by thermal inertia effects but rather was determined by the interfacial contact resistance. The fact that contact pressures were low, on the order of 1 to 5 psi, was largely responsible for poor interfacial transfer. Contact conductance values averaged about 300 BTU/hr-ft^2-^{o}F in ultra high vacuum. Application of soft metallic coatings to the belt and drum units was found to increase the conductance values. Work on all aspects of the design are continuing under Air Force sponsorship (Reference 52).

D. REACTOR APPLICATIONS

The greatest number of investigations of interfacial heat transfer related to a specific application are in the area of nuclear reactor fuel element technology. The fuel elements, generally cylindrical in shape are constructed with a low neutron absorption metallic sheath encasing the fuel. The heat flux levels across the interface between the fuel and the sheath are very high ranging up to about 5.0×10^5 BTU/hr-ft^2. Under these conditions moderate interface resistances can have serious effects on fuel element performance. The heat transfer coefficient on the coolant or working fluid side of the sheath can readily be determined while the contact conductance coefficient adjacent to the fuel surface is difficult to estimate for several reasons. First, it is very difficult experimentally to measure contact conductance values across cylindrical surfaces. Second, proper application of data measured in the conventional manner with flat surface specimens is difficult due to such factors as differential thermal expansion and heat flux variations with fuel burn up. Third, the fuel may be in the form of an enriched refractory oxide which produces inherently low interface conductances and which deforms mechanically in a very complex fashion under thermal cycling.

The difficulties involved are exemplified in a study by Brutto (Reference 53) who conducted contact resistance measurements with cylindrical metal surfaces using copper to simulate the fuel. The contacts between the aluminum and zircaloy canning materials and the simulated fuel were mechanical in nature, no metallurgical bonding being used. Contact conductance values over 20,000 BTU/hr-ft^2-^{o}F were measured and there was some evidence of fusion during the tests. However, it was impossible to estimate the loading across the contact interface with the geometries employed.

As in space vehicle applications one of the important objectives in reactor fuel interface design is to make the contact resistance as low as possible. An additional problem which has not been as difficult to resolve in space vehicle systems is estimating the interface resistance in the first place and determining its variation during reactor operation. As pointed out by Wheeler who conducted extensive investigation on interface resistances in support of the Hanford reactor developments, "thermal resistance of the contact between the core and the jacket of unbonded fuel elements may easily be the largest source of error in core temperature predictions". (Reference 54)

Boeschoten discussed various approaches for improving fuel-sheath heat transfer across a uranium-aluminum joint (Reference 55). The use of high conductivity gases in interfacial voids was not effective since most of the heat appeared to flow across the solid-solid contact spots. Solid lining such as graphite gave only limited improvement. It was concluded that compressive loading or the use of a liquid lining of low neutron absorption cross-section such as sodium, bismuth or tin were the most promising methods of increasing the interfacial transfer. Recently Fenech and Rohsenow (Reference 56) have estimated the interfacial conductance between uranium metal fuel rods and various canning materials including stainless steel, zirconium,

zircaloy 2, columbium, beryllium, aluminum, and magnox A-12. With helium occupying the interface voids, contact conductance values averaging 8000 BTU/hr-ft^2-^{o}F were calculated, with NaK alloy values as high as 1.0×10^6.

Investigations at the MIT Heat Transfer Laboratory under AEC sponsorship were initiated to develop a generalized procedure for the prediction of contact conductances based on physical and geometrical characteristics of the fuel-canning contact members. The method developed accounted for heat flow across both the solid-solid contacts and the void area and was applicable to planar interfaces (References 56, and 57). Because of calculational complexities involved in estimating the required surface parameters an analog computer technique was perfected to perform the necessary computations (References 58, 59, and 60). Important aspects of the analytical formulation will be discussed later. During the course of the work at the Heat Transfer Laboratory experimental investigations were conducted on stainless steel contacts (References 5, 56, and 58), Armco Iron-aluminum contacts (Reference 56), and tungsten-graphite contacts (Reference 59).

A large percentage of recent work on fuel element contact conductance problems has involved the measurement of the heat transfer across flat contact of uranium, uranium dioxide and various canning materials. Variations in the gas present in the interface voids has been an important parameter in most cases. Many have simply reported conductances as a function of compressive load, temperature level, surface finish and interface gas pressure. Important aspects of analytical correlations, related to reactor applications where they have been attempted, are discussed in Sections III and IV. Table II gives a summary of the interfaces studied in support of reactor applications.

E. ELECTRICAL POWER AND THERMAL MEASUREMENT APPLICATIONS

The earliest interest in contact resistance of an electrical nature was associated with the design of switches where it was desirable to minimize Joule heating across the contact. Several references on various aspects of the subject including both static and sliding contacts are available (References 72, 73, 74, 75, and 76). Since vector field equations of the same form govern both electrical and thermal energy transfer across a constriction in an isotropic medium, electrical measurements have been often used in studying thermal contact resistances. The major problem encountered in this approach is that the analogy is valid only for clean interfaces, the electrical and thermal conductivities of contaminating films being widely different.

More recently the wide interest in the design of devices for thermoelectric power applications has resulted in increased interest in the thermal and electrical resistances of semiconductor-metal contacts (Reference 77). As pointed out by Epstein (Reference 78), three factors are important in limiting the efficiency of thermoelectric devices:

(1) Electrode compatibility

(2) Output stability during operation

(3) Contact resistance

The contact resistance produces dissipative Joule heating which of course can have significant effects on performance (Reference 79). This same effect can lead to

TABLE II

SUMMARY OF CONTACT RESISTANCE STUDIES IN THE AREA OF REACTOR APPLICATIONS

Interface Component / Interface Component	Aluminum	Magnox	Zircaloy	Uranium Dioxide	Steel
Uranium	Vacuum (1, 2, 66) Air (66, 67) Helium (2) Liquid Metals (55) Solid Powders (55)	Vacuum (61, 65) Argon (61, 65) Helium (61, 65)			Vacuum (1, 2) Helium (2)
Uranium Dioxide	Vacuum (2)		Vacuum (2, 62) Argon (62, 119) Helium (3, 119) Krypton (63, 119) Xenon (62, 119)	Vacuum (2)	Vacuum (2, 63) Argon (63) Helium (2, 63) Neon (63)
Aluminum	Vacuum (1, 2, 70) Air (68, 69, 70)		Vacuum (2) Helium (2)		
Steel					Vacuum (1, 68, 70) Air (68, 69, 70) Carbon Dioxide (68) Helium (70) Hydrogen (69) Nitrogen (68)

errors in the measurement of the thermoelectric parameters (Seebeck coefficient, α, thermal conductivity, k, and electrical resistivity, ρ) and in turn the thermoelectric figure of merit, $\alpha^2/k\rho$ (References 79, and 80).

There have been some instances where the constriction of a flow field in a material has been used as a basis for transport property measurements. It is clear from Equation 2 that if the constriction resistance can be measured directly, it is then possible to calculate the thermal conductivity in a simple manner. The same is true for the electrical analogy. Cutler (Reference 80) has applied the method for high temperature measurements of the thermal and electrical conductivity of tantalum. A physical constriction or necked down section was machined in the bar specimen with potential probes being mounted on either side.

A variation in geometry still utilizing the constriction phenomena was used by Cutler for very small specimens. Heat generated by an electric current was caused to flow across the small specimen area (constriction) into a much larger heat sink, the temperature drop being measured indirectly from the electrical resistance charge. Based on Equation 2 the ratio of the temperature drop to the heat flux is then proportional to the product of the specimen conductivity and the radius of the constriction.

The thermal comparator developed by R. W. Powell (Reference 81) is a thermal conductivity measuring device which utilizes the principle of constricted flow and which, in the words of the inventor, "gives quantitative expression to the qualitative difference in 'coldness' commonly experienced when handling at room temperature materials covering a range of thermal conductivities" (Reference 82). The method consists in measuring the temperature differential generated when one of a pair of metal spheres, initially at the same temperature is brought in contact with the specimen at a lower temperature. When the geometry of the sphere-specimen contact remains constant the temperature differential between the two spheres is proportional to the square root of the thermal conductivity of the specimen. The device has been used effectively over wide ranges of specimen conductivity from copper to rubber. It is clear that the comparator can be regarded as a system of two semi-infinite solids at different temperatures in contact over a small circular area. It is shown by Clark and Powell (Reference 82) that in the absence of surface films the constriction resistance is given by Equation 2 and thus the governing equations are the same as those in the Cutler small area contact method. Powell and his associates have shown that the method may also be used to study contact resistance, surface roughness, the effective area of contact and its variation with load, and in determining the thickness of foils and surface deposits (References 81, 82, 83, and 84).

SECTION III

ANALYTICAL ANALYSES - SINGLE CONTACT CASE

From the discussion in the foregoing section it is clear that the engineering use of contact conductance data is limited by the sensitivity of this parameter to the physical and chemical condition of the contacting members, the compressive loading and complicating effects induced through such variables as thermal cycling. Highly empirical studies to establish broad ranges of contact conductances expected for practical joints has been an accepted approach since analytical prediction procedures may be complex and often lack generality. Thus, even though it is recognized that factors such as surface characterization are very important when studying the mechanics of interface energy transport, inattention to the analyses of these is not necessarily an error of omission for engineering applications.

Since 1948, however, emphasis has been placed as much on analytical analyses which allow quantitative prediction of contact conductance as on the generation of practical data on interfaces likely to be encountered in practice. Even though some of these prediction procedures are difficult to use, they have lead to semi-quantitative or in some cases, completely explicit methods of predicting contact resistance in terms of the more important independent variables. A review of these analytical developments is presented in the next two sections. These analyses usually begin with consideration of the characteristics of the single contact, and the derivation of the constriction resistance equation.

If it is assumed that there are N solid-to-solid contact spots per unit superficial area of contact, and that these true contact spots are uniformly distributed and of equal size, then each of the contacting members can be divided into N imaginary elementary cylinders transferring no heat to one another, each containing or "feeding" one solid spot. The sketch in Figure 1b indicates that this approximation has some physical justification. The analysis then reduces to consideration of one of these "contact elements" and determining the additional resistance imposed by constricting flow to the area of the solid spot when moving from one elementary cylinder to the other across the interface. Figure 3a presents a cross-section of the element under consideration; 'b' is the radius of the "feeder" contact element and 'a' the radius of the circular, solid-solid contact.

The classical electrical analogy of determining the "constriction resistance" induced in an electrical conductor exhibiting a discontinuous reduction in cross-section, Figure 3a, was worked out many years ago by Kottler (Reference 85) as recently discussed by Holm (Reference 86). As indicated in Figure 3b, the flux lines are approximated by a family of hyperbolic curves, the orthogonal equipotential surfaces then being elliptical in shape possessing common foci with the flux curves. The final result of the calculation is given in Equation 2a

$$R_c = \frac{\rho}{2a} \tag{2a}$$

where,

R_c = constriction resistance

ρ = electrical resistivity of the solids

a = contact radius

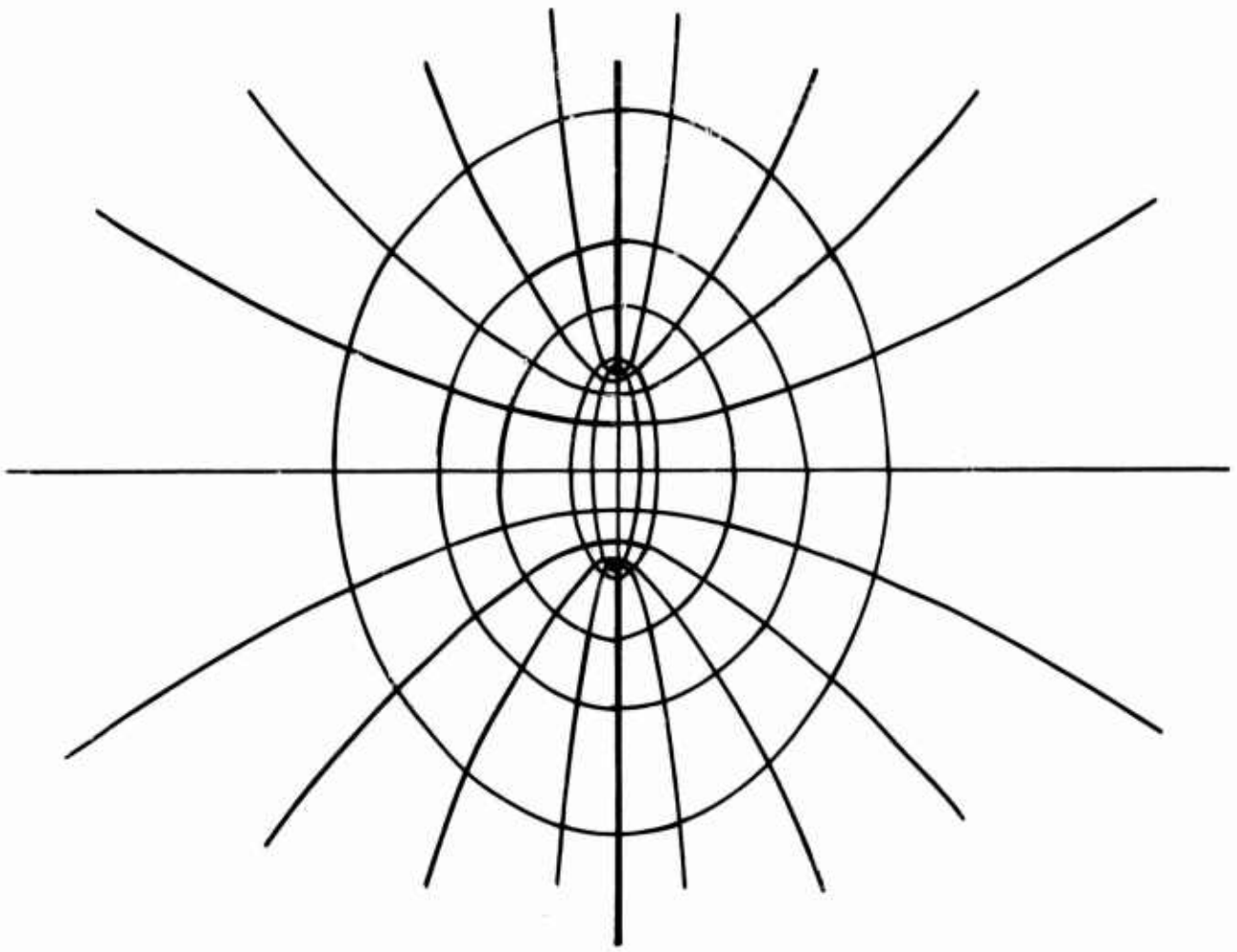

Figure 3b. Flux Lines Near a Circular Constriction

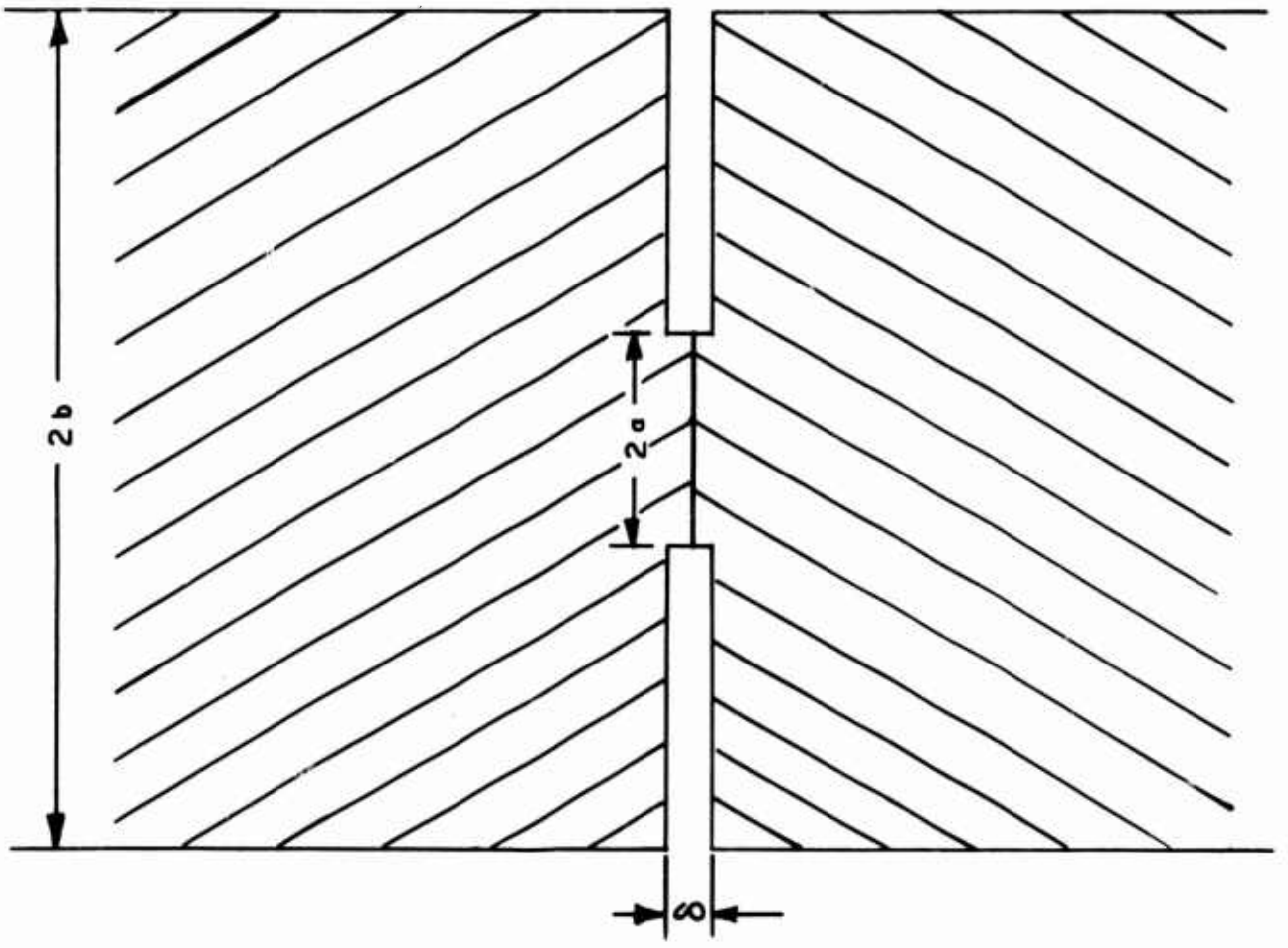

Figure 3a. Elementary Contact Element

An expanded treatment of essentially the same problem related specifically to the thermal contact case was carried out by Centinkale and Fishenden (Reference 87). In their analysis, some heat flow across the fluid gap ($a \leq r \leq b$, Figure 3a) is allowed as well as across the solid contact area. The problem involves solution of the Laplace equation,

$$\nabla \cdot (k \nabla T) = 0 \tag{3}$$

with a potential field distribution nearly the same as that shown in Figure 3b. In general from elementary potential field theory, if a potential function ψ is defined, then the resistance to flow between any two equipotential surface elements ψ_1, and ψ_2 is given by,

$$R = \frac{\text{potential difference}}{\text{flux density}} = \frac{|\psi_1 - \psi_2|}{k \int_{A_1} \left| \frac{\partial A_1}{\partial n} \right| dA_1} \tag{4}$$

where,

k = thermal conductivity

ψ = potential function

A = cross section of "stream tube" bounded by constant flux lines

$\frac{\partial}{\partial n}$ = normal differential

A geometric schematic of the equipotential surfaces (isotherms) in the proximity of the thermal contact is given in Figure 4. The dividing flow line separates the heat which eventually flows through the solid and fluid parts of the resistance. The dotted isotherm would coincide with the plane $z = 0$ if there were no gap between the solids. Thus, the solid resistance introduced by the gap is that between this isotherm and the plane $y = 0$. As in the case of the electrical constriction resistance (Figure 3b) this field is approximated by elliptical isotherms with their foci at $x = \pm a$.

Using Equation 4, the solid resistance is expressed geometrically as

$$R_s = \frac{1}{k} \int_0^{W_0} \int_0^{a} \frac{\text{distance between AB and CD}}{\text{area generated by AB}} \, dV\,dW \tag{5a}$$

$$R_s = \frac{1}{K} \int_0^{W_0} \frac{dW}{a^2 + W^2} \Bigg/ \int_0^{a} \frac{V\,dV}{\sqrt{a^2 - V^2}} = \frac{1}{2\pi a k} \tan^{-1}\left(\frac{X_d - a}{a}\right) \tag{5b}$$

If $(x_d - a) \to \infty$ (i.e., Figure 3b) Equation 5b reduces to Equation 2a when $(1/\rho)$ is replaced by k. (Equation 5b must be multiplied by two to account for the fact that each contact is made up of two members).

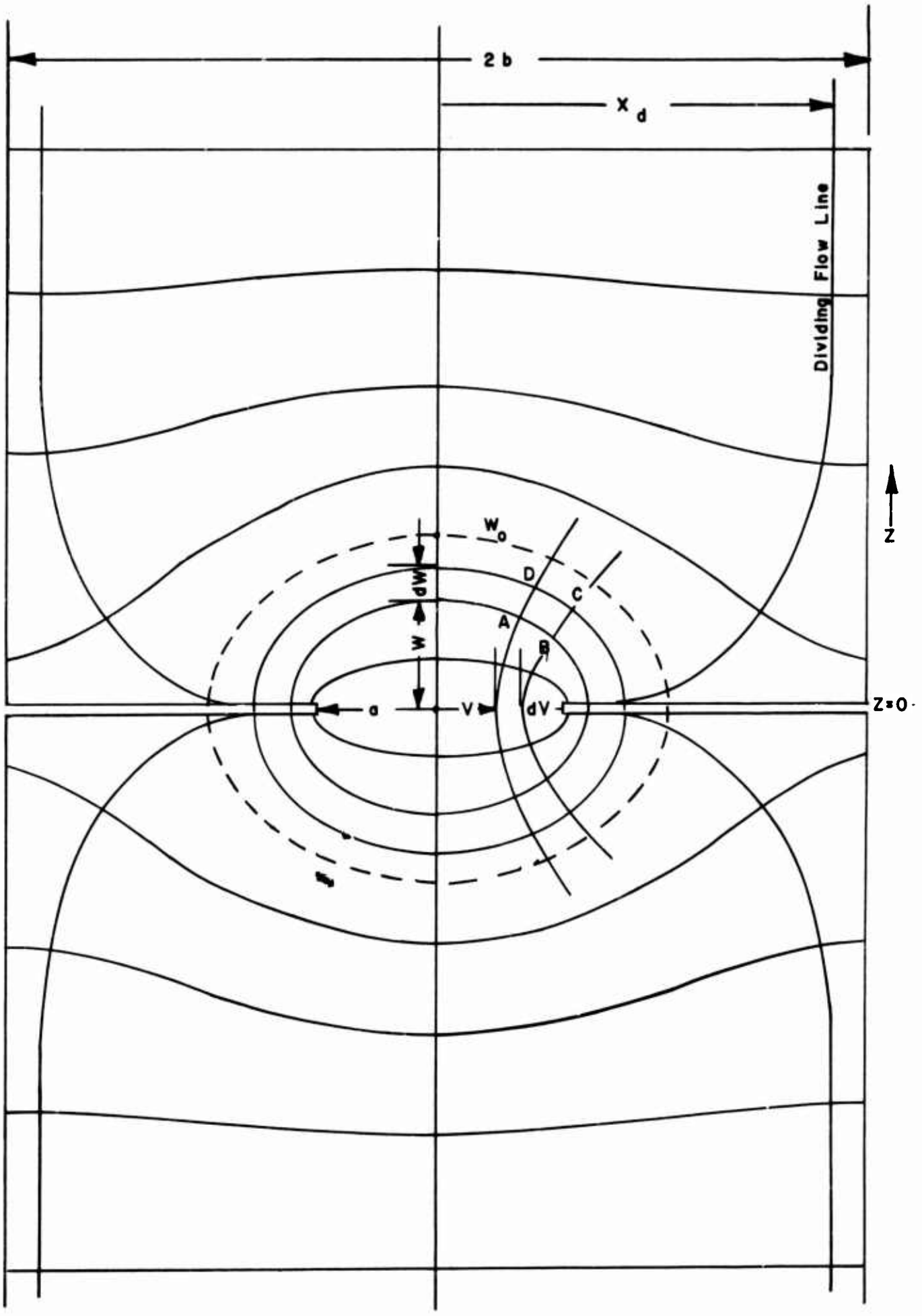

Figure 4. Flux - Potential Distribution for a Single Contact

The above problem can be handled in exact terms, of course, because the potential function may be written explicitly. Similiarly if the heat flow through the fluid is assumed to be linear the following simple expression for the fluid or gas phase resistance results.

$$R_g = \frac{\delta}{\pi b^2 K_g} \tag{6}$$

Values of R_s and R_g calculated from the above equations are compared by Cetinkale and Fishenden with values obtained with isotherms established by the Southwell relaxation method. Agreement was within 2 percent for various ratios of a/b and $bk_g/\delta k_s$.

The more general derivation of the constriction resistance equation is obtained by considering the flow of heat between two semi-infinite regions which are at different temperatures and are in contact over an area of radius a. Under conditions where no heat flow occurs across the region $z = 0$, $r < a$ the Laplacian equation is rewritten in cylindrical coordinates and the solution obtained by transform techniques. Applying the boundary conditions, the form of the temperature field becomes (Reference 82)

$$T = T_o \left[1 - \frac{1}{\pi} \int_0^\infty e^{-\lambda z} (\sin \lambda a) J_0 (\lambda r) \frac{d\lambda}{\lambda} \right] \tag{7}$$

In turn applying this result in Equation 8 leads directly to the constriction resistance equation.

$$R_c = \frac{\Delta T}{q} = \frac{\Delta T}{2\pi k \int_0^a r \left(\frac{\partial T}{\partial z}\right)_{z=o} dr} = \frac{1}{2ka} \tag{8}$$

Considering the region in the immediate proximity of the solid conduction channel, if a perfect contact exists as depicted in Figure 3a a necessary boundary condition describing the temperature field is

$$T(r,o) = T_{interface} \quad 0 \le r \le a \tag{9a}$$

If an imperfect contact exists in the region $o < r < a$ the definition of R given in Equation 4 does not hold and in the limit of a high resistance in the region considered, the isothermal boundary condition, Equation 9a is replaced by a constant heat flux boundary condition,

$$-k \frac{\partial T}{\partial z} (r, 0) = q, \quad 0 \le r \le a \tag{9b}$$

Holm (Reference 86) has shown that for this constant heat flux case the "1/2" in Equation 2a is replaced by $(1/\pi)$ based on the temperature at the center of the contact. Thus, there appears to be about a 25 percent difference in the calculated value of R_c for the two cases. However, Clausing and Chao (Reference 88) point out that evaluation of the constant heat flux case should be carried out with a variable radial temperature along the plane $z \pm 0$ rather than using the maximum center line value assumed by Holm. Temperature distribution data giving $T = f(r)_{z=0}$, $0 < r < a$ for

different heat flux levels were obtained by Roess (Reference 89); using this relationship Clausing and Chao performed the evaluation of R_c by numerical integration. The results indicated that Equation 2a is valid for both boundary conditions, Equations 9a and 9b.

The next important consideration to be discussed in relation to the characteristics of the simplified model in Figure 3a is the case where "a" increases until it becomes comparable to "b". Physically this would be the case encountered at very high loads or with very smooth surfaces. Qualitatively the N adiabatic rods into which the contact members were originally divided no longer are truly isolated but interact with a net reduction of the constriction resistance. This effect has been termed "constriction alleviation" and has been expressed in terms of the ratio x = a/b. An analog study of the case where a constant potential circular spot of radius "a" feeds a coaxial cylinder of radius "b" yields the following result for the constriction alleviation factor g(x),

$$g(x) = 1 - 1.0925\,x = 0.29591\,x^2 = 0.05254\,x^5 + \text{----} \qquad (10)$$

There is experimental evidence, mainly from liquid analog studies conducted by Clausing (Reference 88), that this expression holds fo $x \leq 0.65$. A more generalized form of Equation 2a then becomes

$$R = \frac{g(x)}{2ak} \qquad (11)$$

Laming (Reference 90) has concluded that at loads ranging from 2000 to 8000 psi on fairly rough metallic interfaces (150-1500 μ in.) significant constriction alleviation effects are observed.

The length, L, of elementary heat conduction channel (r = b) does not influence the value of R_c for L/b greater than 1.0. The effect, if present, is greatest for values of x near unity. An important correllary to this observation is that the axial distance from the interface in which the temperature field is perturbed as a result of imperfect contacts is on the order of separation of the surface asperities.

The other basic method of analyzing the heat transport in the simplified one-contact model presented in Figure 3a is carried out by rewriting the Laplacian equation in cylindrical coordinates and solving the resultant zero-order Bessel equation with appropriate boundary conditions. The simplest approach using this method is to assume zero heat flow across the void area as was done by Clark and Powell (c.f. Equations 7 and 8). If heat transfer across the void area is allowed, the solution procedure is somewhat more complex. Fenech and Rohsenow (Reference 57) have derived equations for this case by making several simplifying approximations. First, the idealized contact was divided into several regions as shown in Figure 5a. The solution of the steady state conduction equation, $\nabla^2 T = 0$ in each region was then by the method of separation of variables. Explicit solution of the problem is only possible if average boundary and coupling conditions are written for the various regions along with the assumption of pure axial conduction through the fluid gap and in the cylindrical contact region of radius a and height $\delta_1 + \delta_2$. Only the more important steps of the lengthy solution will be included here. A representative average boundary condition is given in Equation 12a, while the axial flow coupling condition between the contact members and the fluid in the void or gap is given in Equation 12b,

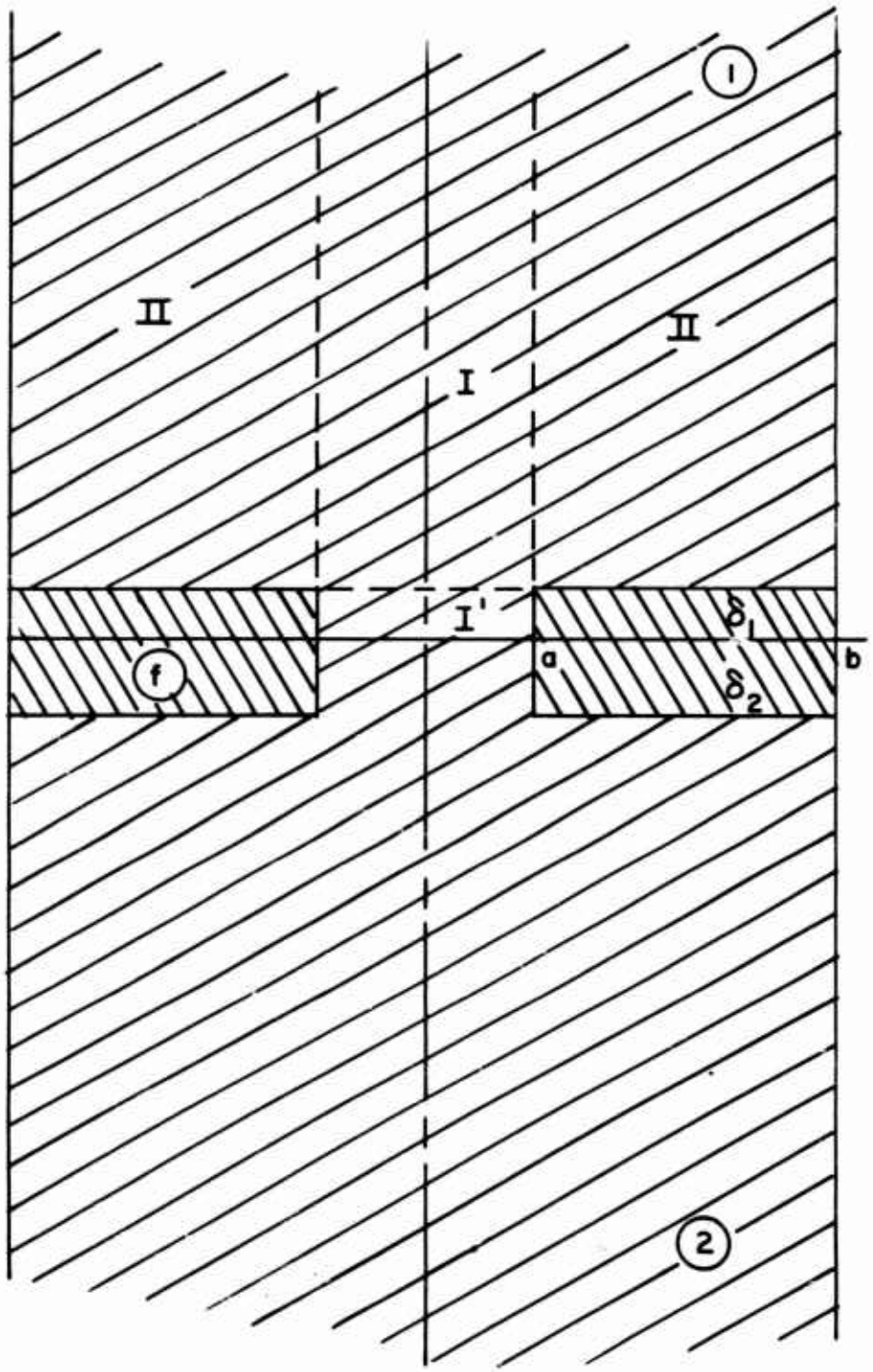

Figure 5a. Idealized Multi-zone Contact

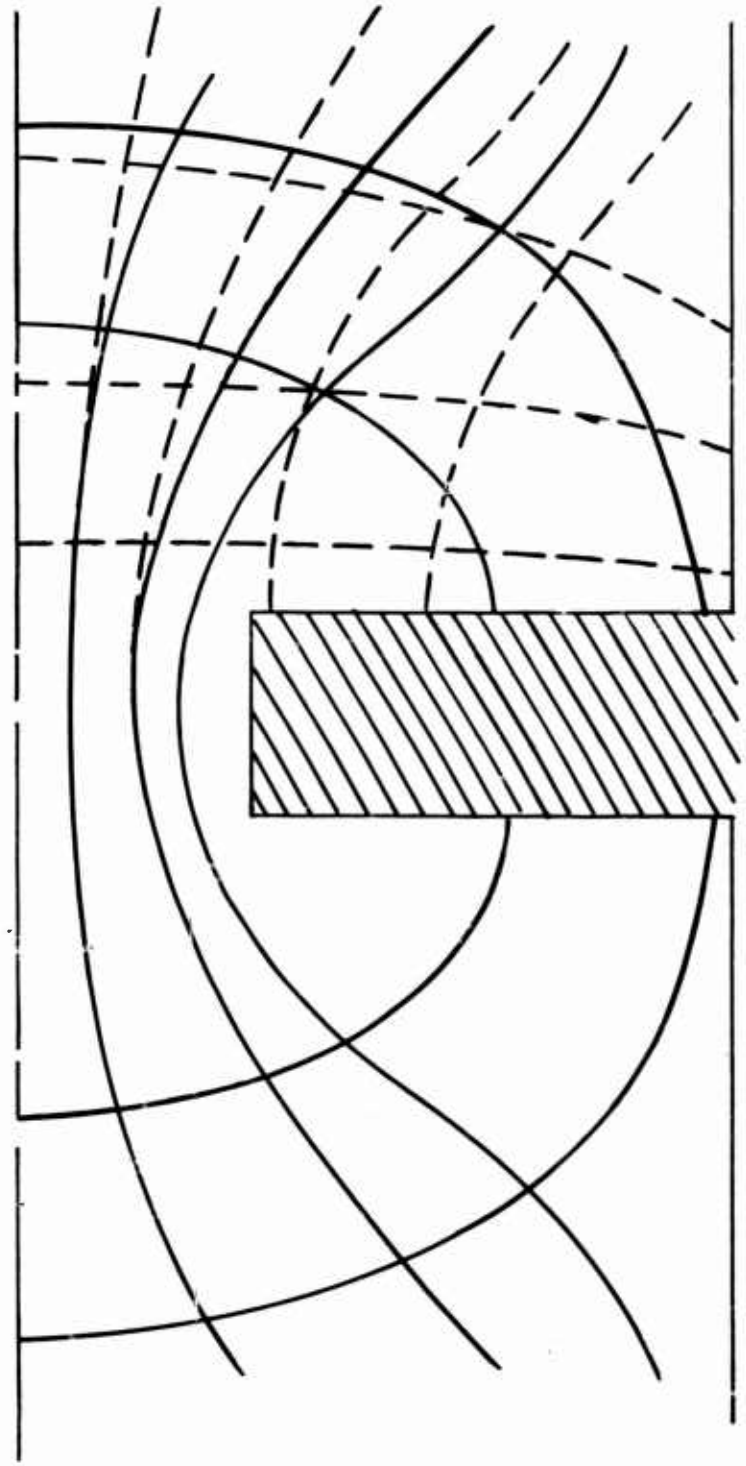

Figure 5b. Distortion of Temperature and Heat Flux Field as a Result of Assumed Boundary Conditions

$$z = 0,\ 0 < r < a,\ \int_0^a (T_I' - T_0)\, r\, dr = 0 \tag{12a}$$

$$a < r < b,\ \int_a^b k_1 \left.\frac{\partial T_1}{\partial z}\right|_{z=\delta_1} r\, dr = -\int_a^b k_2 \left.\frac{\partial T_2}{\partial z}\right|_{z=\delta_2} r\, dr = \int_a^b k_f \frac{(T_1 - T_2)}{\delta_1 + \delta_2}\, r\, dr \tag{12b}$$

A solution of the form given in Equation 13 for the region I is assumed.

$$T_I = T_0 + g(z+d) + A J_0(\alpha r)\, e^{-\alpha z} \tag{13}$$

where,

J_o = Zero order Bessel function of the first kind

A, α = Constants

The factor gd is essentially a "temperature displacement" term which arises from the contact disturbance. Thus, the external solution $T_o + g(z+d)$ tends to the temperature $T + gd$ as $z \to 0$ rather than to T_o. Based on the definition of the interfacial conductance, we have the following,

$$h_c = \frac{1}{R} = \frac{\left(\frac{q}{A}\right)}{\Delta T_{interface}} = \frac{1}{\frac{d_1}{k_1} + \frac{d_2}{k_2}} \tag{14}$$

Evaluation of the temperature displacement terms is quite involved, however, the final solution is in the form of a sum of two terms

$$q_{total} = q_{solid} + q_{void} = \frac{\pi a^2 (T_1 - T_2)}{\frac{\delta_1}{k_1} + \frac{\delta_2}{k_2}} + \pi (b^2 - a^2)\, \frac{k_f (T_1 - T_2)}{\delta_1 + \delta_2} \tag{15}$$

hence,

$$h_c = \frac{\frac{q}{A}}{T_1 - T_2} = \frac{\frac{k_f}{\delta_1 + \delta_2} (1 - x^2) \left(\frac{\delta_1}{k_1} + \frac{\delta_2}{k_2}\right) + x^2}{\frac{\delta_1}{k_1} + \frac{\delta_2}{k_2}} \tag{16}$$

where,

$$x = \frac{a}{b}$$

Added terms from the analytical solution which describe exactly the temperature-heat flux field corresponding to the assumed boundary and coupling conditions are included in an equation similar in form to Equation 16.

Physically, the differences between this model and that discussed earlier are sketched out in Figure 5b. Coupling conditions of the form given in Equation 12b cause the heat flux lines (dotted curves, Figure 5b) to have a steeper slope near the constriction so that the heat flux through the solid and void areas in the region $x = \delta$ are directly proportional to k_s and k_f respectively. This in turn requires that the plane $z = \delta$ be isothermal which of course could be a rather questionable approximation. The isotherms are in turn more flat and less distorted than in the true physical case. Some flattening in the actual isotherms would be expected because of heat flow through the voids but not to the extent forced by the analysis. Fenech and Rohsenow indicate that their somewhat limited experimental data has shown the initial approximations to be of no serious consequence.

The results of the boundary value solution of Fenech and Rohsenow can be compared with the basic constriction resistance equation, Equation 2a, by reducing the equation to the case where $k_1 = k_2$ and the void phase conduction is zero (Reference 91). The result is

$$R_c = \frac{1}{h_c} = \frac{2.4\,\frac{\delta}{a} + 2}{2.4\,\pi\,ak} = \left(\frac{1}{1.7\,ak}\right)_{\delta \cong a} \tag{17}$$

The equivalent constriction resistance is then slightly greater than that given by Equation 2a when δ is on the order of a.

If either of the above approaches are to be used successfully in analysis of thermal contact resistance phenomena where solid and gaseous conduction are the predominant modes of interfacial heat transfer, the characteristics of the contacting surfaces must somehow be reduced to expressions involving the parameters a, b, and δ. This is where the real problem arises in correlations between experimental data and analytical predictions. To date, only very marginal success has been realized, mainly on physically elementary surfaces. When the main experimental variable is the compressive load, the surface parameters a, b, and δ become complex functions of the elastic and plastic mechanical characteristics of the mating materials. Since real surfaces may exhibit several types of surface roughness and waviness, definition of geometrical surface characterizing parameters often becomes a difficult or impossible task in itself. Surface contamination, low conductivity surface films, and radiation heat transfer contributions are complicating influences which may be of importance.

SECTION IV

CONTACT RESISTANCES ANALYSES OF REAL MULTIPLE CONTACT INTERFACES SURFACES

A. GENERAL APPROACH

Starting with a relationship of the form of Equation 11, the simplest expression for "a" in terms of physically measurable quantities is obtained as follows. Assuming N circular solid-solid contact spots, the total solid-solid contact area A_s is

$$A_s = N \pi a^2 \tag{18}$$

If it is argued that the loads which can be supported by elastic deformation are extremely small, then it can be assumed that the pressure over each solid-solid contact spot is equal to the yield pressure of the contact members (the yield pressure of the softer material if the contact is made up of different materials). The yield pressure is nearly equal to the Meyer hardness, H_m. Thus, if the load on the contact is L, the applied pressure, ρ , and the total area A_T,

$$L = H_m A_s = P A_T \tag{19a}$$

or,

$$a = \left(\frac{1}{N\pi} \cdot \frac{P}{H_m} \right)^{1/2} \tag{19b}$$

Substituting in Equation 11,

$$R_{solid} = R_s = \frac{g(x)}{2k} \left(\frac{\pi}{N} \cdot \frac{H_M}{P} \right)^{1/2} \tag{20}$$

In cases where solid-solid conduction predominates, and where the simplifying assumptions concerning the use of the Meyer hardness are valid, the contact resistance should vary as $L^{-1/2}$. If the contact interface is subjected to extremely low compressive loads or if the surfaces are very smooth, the deformation could possibly be elastic. In this case the classical Hertzian elastic deformation equation for the solid-solid contact area (Reference 92) can be applied,

$$a = \left[\frac{3}{4} L \left(\frac{1-\mu^2}{E_1} + \frac{1-\mu^2}{E_2} \right) \left(\frac{1}{r_1} + \frac{1}{r_2} \right)^{-1} \right]^{1/3} \tag{21}$$

where,

μ = Poisson's ratio

E = modulus of elasticity

r = radii of contacting asperities

Hence in the case of elastic deformation the contact resistance becomes proportional to $L^{-1/3}$ for the simple case assumed. The discussion concerning the validity and

limitations of Equation 20 falls logically into two areas: first, the deformation characteristics of the surfaces in contact associated with the term H_M; second, the geometrical characteristics of the surfaces involved in the evaluation of N. These are considered separately as follows:

B. SURFACE DEFORMATION CHARACTERISTICS

In estimating the true solid-solid contact areas as a function of compressive load, a correction to Equation 19a is often employed as follows,

$$A_s = \frac{L}{\xi H} \tag{22}$$

where,

H = hardness, (Vickers, Meyer, etc.)

ξ = empirical deformation factor

If full plastic flow is initiated, with no complicating factors such as work hardening, then $\xi = 1$ and the area available for direct solid conduction, A_s, will be the applied load divided by the Meyer or Vickers hardness. These hardness values should be employed since they are defined in terms of the projected area of the indentation rather than the total area. The projected area is, of course, that available for heat transfer. In actual cases, many complex factors lead to values of $\xi < 1.0$; these will be discussed further. Generally $1/3 < \xi < 1$ since both work hardening and elastic deformation may be significant.

If a plot of mean yield pressure, P_m, as a function of load is made for a typical metal undergoing compression, the curve in Figure 6 would be obtained where the Y is the elastic limit of the metal in tension. The deformation is elastic up to about $P_m = 1.1$ Y., 0 to x, Figure 6. Plastic flow is fully initiated when $P_m \cong 3.0$ Y. Beyond this point (y to z, Figure 6) the mean pressure on the contact surface is constant and the contact area becomes directly proportional to the load. Since hardness, H, is defined as the load per unit area of real contact, the following important relationship can be written for the plastic flow region in Figure 6,

$$H = \frac{L}{A_s} = P_m \cong 3Y \tag{23}$$

In hardness measurements with spherical indenters the nature of the deformation is related to the size of the indentation; empirically it has been shown that the percentage of strain or deformation of the indentation edge is given by the factor (20 d/D), where d = indentation diameter, D = indenter diameter (Reference 93). Full plasticity is reached when $d/D \geq 0.1$ or at strains greater than 2 percent. For conical and pyramidal indenters, full plastic flow is initiated immediately when the point touches the surface. In the case of the pyramidal Vickers indenter the strain is approximately constant at about 8 percent (Reference 94); hence, it is possible to estimate the Vickers hardness from stress-strain characteristics of the material. In this case, as opposed to the case with spherical indenters, the hardness should be independent of the load and indentation size according to Equation 23. For work in contact resistance then Vickers and Meyer hardness values have more physical significance than Rockwell or Brinnell values which are obtained with spherical indenters.

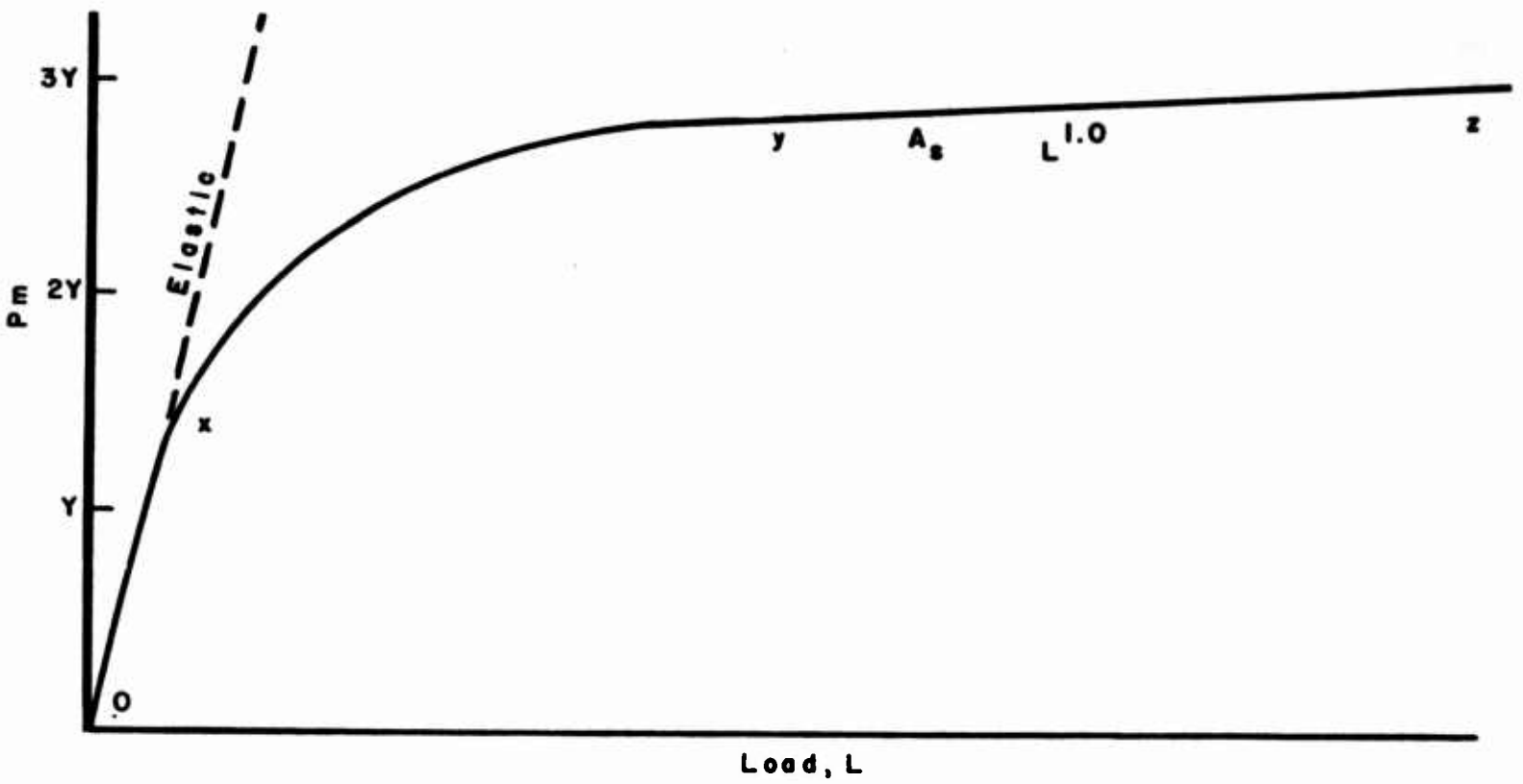

Figure 6. Yield Pressure as a Function of Load

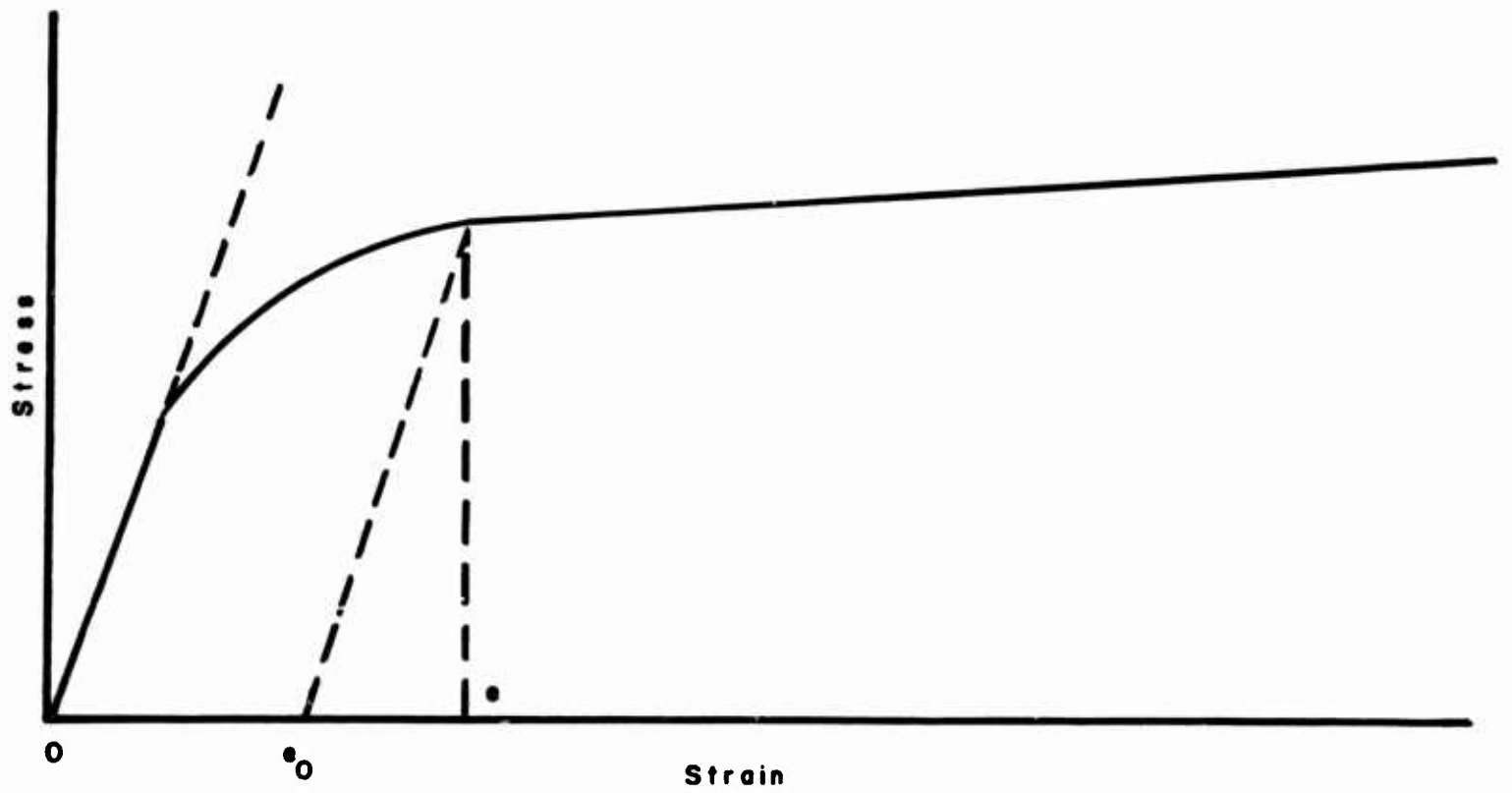

Figure 7. Stress-Strain Characteristics of a Real Metal

For annealed materials that work harden the elastic limit, Y, increases with deformation and the area of contact, A_s, is proportional to $L^{4/5}$, whereas for fully worked material $A_s \alpha L^1$. Referring to Figure 7, two characteristics of partially worked metals are of importance in determining deformation under cycling loads. If the material has been brought to a state with strain = ϵ, on removal of the load it will recover elastically to a condition with residual strain ϵ_o. The modulus of the material is little affected by work hardening, thus the slope of the dotted curve in Figure 7 is essentially the same as the slope of the curve in the elastic region near the origin (0 to X). Because of the deformation ϵ_o the yield stress for this material is now much greater than the initial elastic limit. For the fully worked material it will equal the ultimate tensile strength. A cross plot of contact area as a function of load is given in Figure 8 for a typical cycling compression. For a surface where the load is high enough for both the asperities and the substrate to undergo plastic deformation, the mean pressure will be the yield strength of the bulk material. This is because the asperities can support a much greater load due to their more severe work hardening.

Another important observation based on the same behavior is the fact that for partially worked materials, larger indentations are required to produce full plasticity than on the annealed material. Hence, for small indentations in such materials when hardness values based on full plastic flow are used in calculations of contact area considerable error could result. However, in the case of different materials undergoing cyclic compression the harder material will undergo a greater elastic recovery than a soft material and thus the possibly greater surface adhesion between the hard surfaces will tend to nullify differences in hysteresis for interfaces made up of materials with different hardness.

For real metals, it has been observed that the hardness is not indepeudent of load and thus when estimating values of H for contact resistance studies it is necessary to work in the microhardness range where the indentation areas are comparable to the solid-solid contact areas developed between the asperities of contacting surfaces. This range is defined generally according to the following Table (Reference 95).

TABLE III

HARDNESS RANGES

Indenter Load	Hardness Range
10 kgm	Macrohardness
10 kgm - 200 gm	Low-load hardness
1 gm - 200 gm	Microhardness

Both increases and decreases in hardness at low loads have been observed by different investigators on various metals. Although the explanation is yet unresolved, increased apparent hardness with decreasing load is attributed to metallurgical effects whereas decreases in hardness with reduced load is most often attributed to inaccurate or faulty measurement techniques (Reference 96). An increase in both Vickers and Knoop microhardness of stainless steel at low loads has been observed by Henry in the range of solid-solid contact areas found with contacting surfaces (Reference 58).

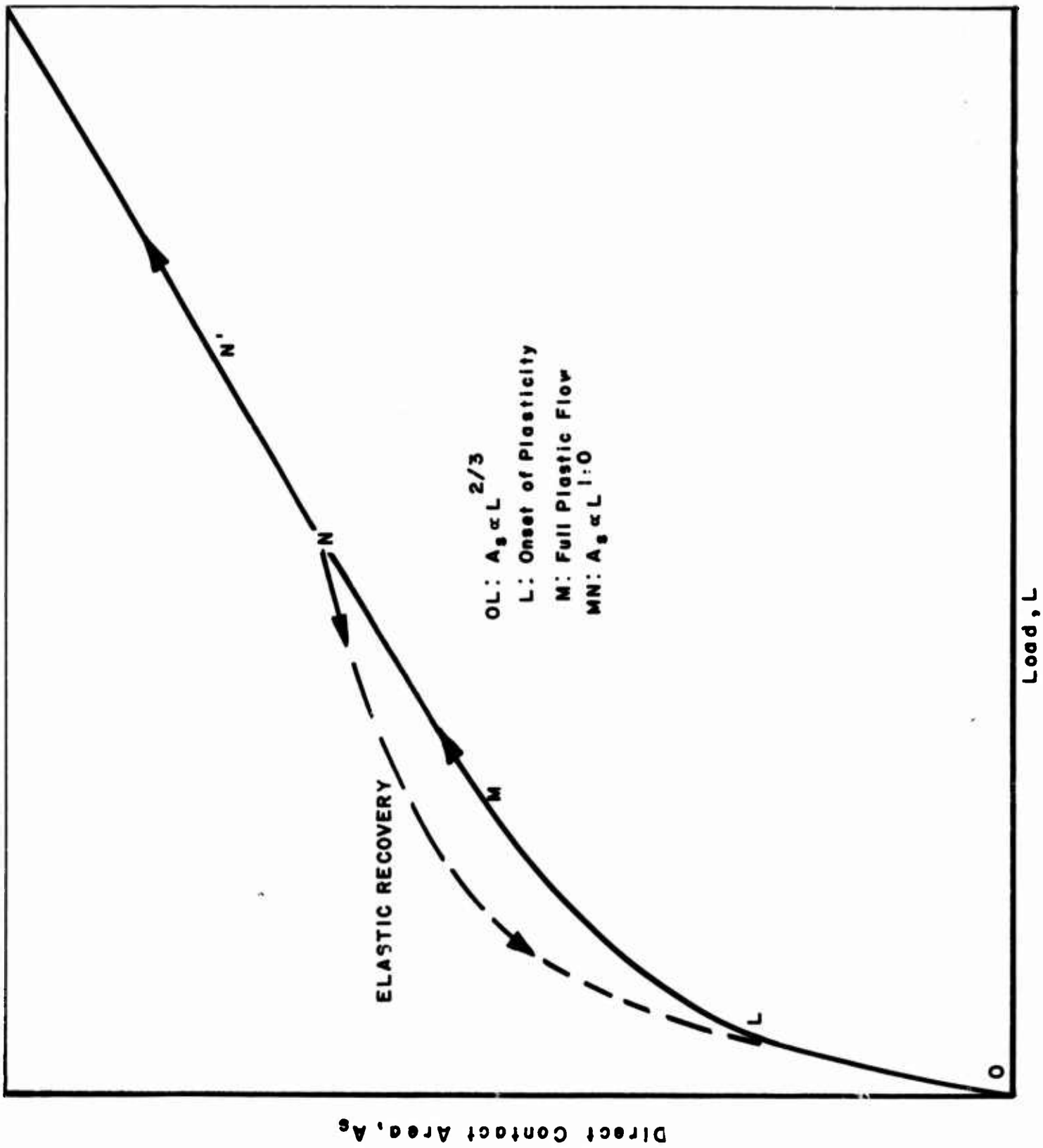

Figure 8. Variation in Contact Area With Load Cycling

Microhardness values of up to $6X10^5$ psi were obtained by Henry as compared with a nominal value of around $3X10^5$. Laming (Reference 90) calculated microhardness values as high as $1X10^7$ psi for mild steel in correlating observed contact resistance data. However, other factors such as surface waviness contributions at low loads may have caused these calculations to be greatly in error. In work on fairly coarse gun metal contacts, Tachibana (Reference 97) found that experimental Brinnell hardness values had to be multiplied by an empirical factor of 2.5 to correlate the experimental contact resistance data when an equation similar to Equation 19 was used to estimate the solid-solid contact area.

The important and also complex role which elastic-plastic deformation contributions make to thermal contact resistance is shown in the extensive empirical work of Cordier, Maimi, and Bory (References 98, 99, and 100). The variability in the observed contact resistance values as a function of load and load-cycle history illustrate that a great degree of caution must be exercised in the estimation of solid contact areas from hardness measurements. The work was conducted with high roughness interface contacts of brass and steel (120 to 1800 μ in.) at loads up to 2500 psi. The results are summarized in Figure 9. The first compression-decompression cycle is outlined by the solid curve in Figure 9a. When the maximum load is maintained for several hours, the contact resistance decreases and then follows the lower solid curve on decompression. All subsequent compression-decompression cycles to load levels below the initial maximum fall within the envelope outlined by the dashed curves (a) - (b), Figure 9a. Figure 9b is an expanded plot of the (a) - (b) envelope with several intermediate load cycles shown. Thus depending on the manner in which a given load level is achieved, the contact resistance can assume any value within the well defined limits, (a) - (b). At least qualitatively these effects are expected from the variation in solid-solid contact area under cyling loads which was discussed in connection with Figure 8.

Once the (a) - (b) envelope had been defined after cycling to a fixed maximum load, various intermediate loads were maintained for extended periods of time to examine relaxation effects. On the compressive leg at a given load, it was found that the contact resistance decreased with time. At the same load on the decompression leg it was found that the contact resistance increased. Since the final two values of the contact resistance reached on the compression and decompression legs at any given load were nearly identical, it was concluded by these authors that only one equilibrium curve, $R_c = f(L)$, existed. The equilibrium curve was unique only at load levels below the maximum experienced by the contact. The compression-decompression envelope was thus attributed to non-equilibrium measurements at the various intermediate loads. "Non-equilibrium" in this context was defined as a compression-decompression cycle extending over a two day period. At any given load level, the equilibrium contact resistance values were attained only after a period of 4 to 5 days.

C. GEOMETRICAL CHARACTERISTICS

Hardness measurements would allow straight forward determination of the solid-solid contact area available for heat transfer if it were not for complicating effects of elastic deformation, work hardening and other factors aforementioned. Since hardness correlations give no information on the size, shape or distribution of the contacts (Reference 21) examination of the geometrical properties of the contact surfaces from visual or photographic observation, profilometer traces or surface sensitive parameters such as specular emittance is often employed to provide additional information relatable to the physical nature of the contact. In general, at least

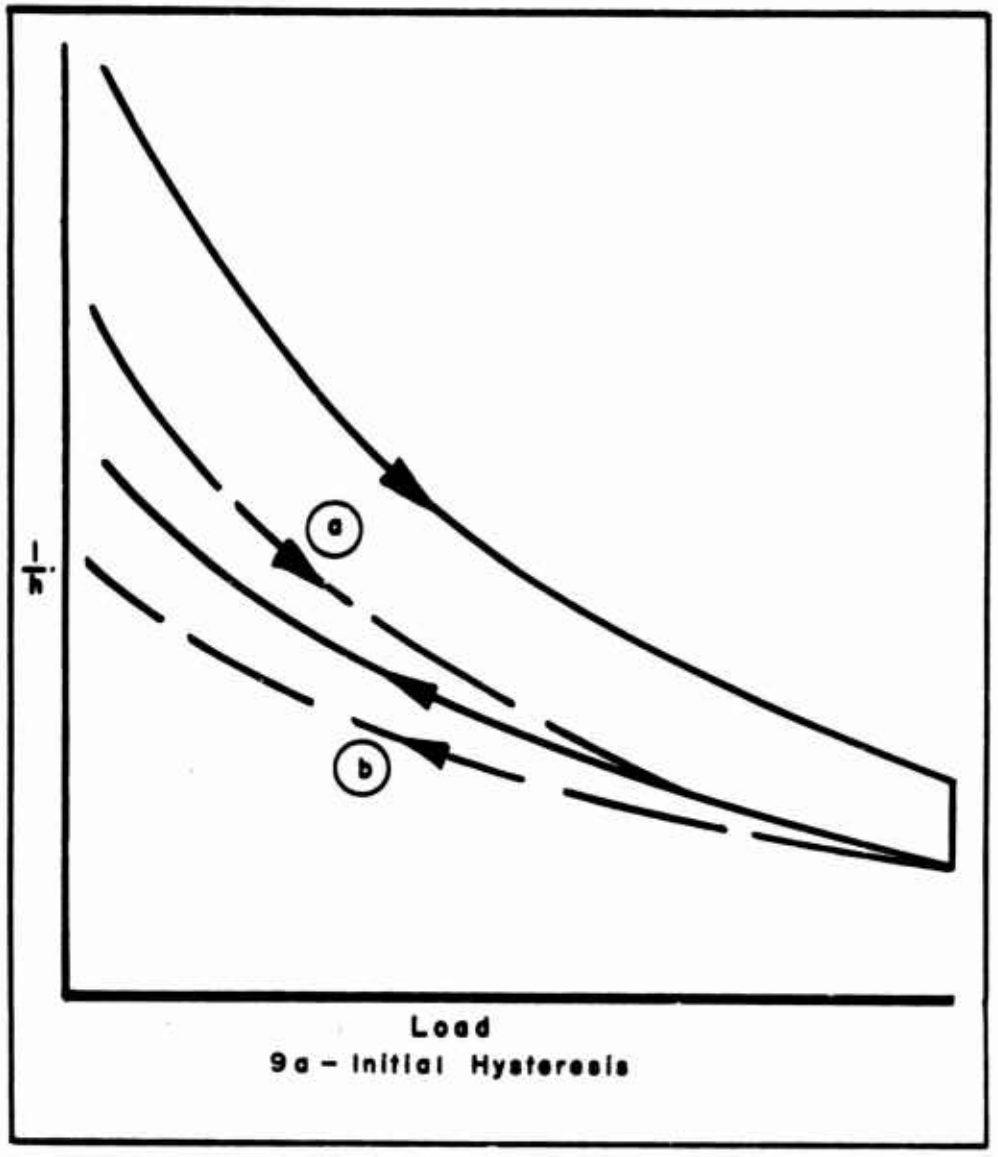

9a - Initial Hysteresis

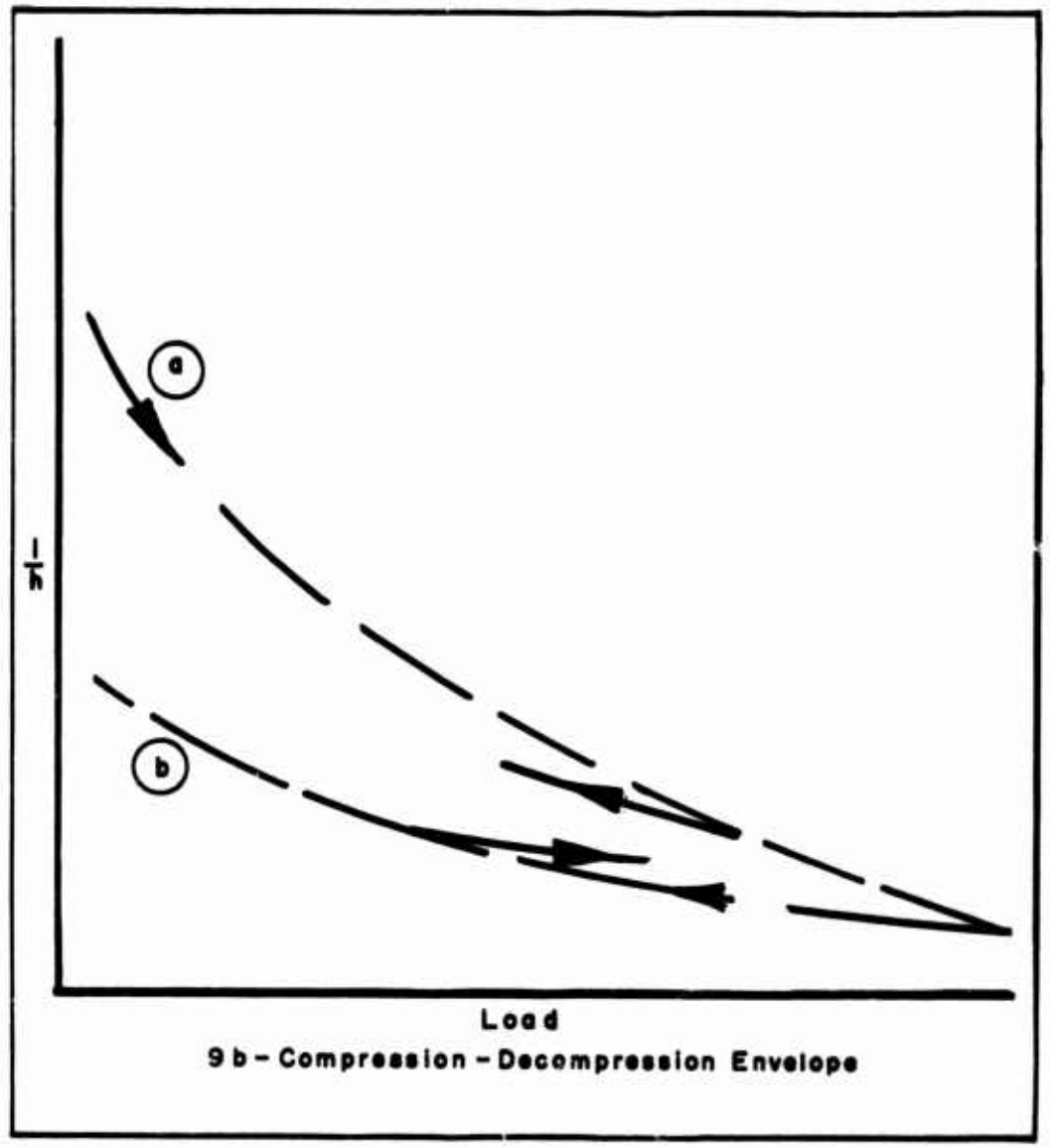

9b - Compression - Decompression Envelope

Figure 9. Hysteresis Effects in Thermal Contact Resistance on Load Cycling

two qualities of nominally flat surfaces, free of gross imperfections and superficial damage: e.g. scratches, pits, must be considered immediately in determining surface characteristics. The first is surface roughness which can be defined as those surface irregularities which are microscopic in nature; the second is surface waviness which can be considered as macroscopic deviations from overall surface flatness.

As with other aspects of thermal contact resistance work there is disagreement as to the proper application of such data in analyzing experimental results. It is intuitive that rough surfaces make poor contact whereas smooth surfaces likely provide better contact and that compressive loading improves the contact in both cases. Beyond this observation, for which qualifications must often be made, very little of a general nature can be said.

Several references are available which describe methods of surface finish analysis and which discuss the types of finishes which can be obtained through various mechanical operations (References 101, 102, and 103) and thus these items will not be discussed further. The following will emphasize the methods of surface property analysis which seem to have been successful in understanding contact resistance phenomena.

Conventional lathe or milling machine operations yield surface contours with a definite lay or directional character (parallel grooves or scratches, concentric circles and the like). If surfaces finished in this manner are brought into contact the nature of the interface is dependent on the relative orientation of the contact members. This is in contrast to an interface made up of specimens with a random lay as might be achieved with a sand-blasting operation. In this instance the character of the interface should be independent of relative orientation of the contact members.

Thus, the nature of the surface finishing process may greatly influence the distribution and number of the solid contacts as a function of load. Through contrast microscopy studies Dyson and Hirst (Reference 104) found that the true area of contact between lapped steel surfaces was made up of a very great number of small contacts which increased in number but not size with increasing load. Polished surfaces of the same specimens exhibited contact uniformity across the macroscopic contact area. In studies with true surface profile traces on roughly milled (150 μ in. rms) iron-aluminum contacts, Fenech (Reference 57) found an increase in both number and size of the contact areas with increasing load. Work hardening effects were not considered, in this analysis. Several authors have observed that the number of solid contacts increases in the same manner with increasing load as the total contact area, the average size of the contacts remaining constant. Results from a series of rough metallic interfaces (400 μ in.) performed by Boeschoten and van der Held (Reference 67) indicated that the average solid contact radius was approximately 120 μ in. (30 μ) independent of load and independent of the metals making up the contact. Through optical determination of contact area as a function of load on transparent plexiglas models Shvetsova (Reference 105) found that both the total area and the number of individual contact points increased linearily with load. Hence the average size of the individual contacts remained constant and was calculated to be approximately 0.020mm^2 (r=3000 μ in.). This value was obtained for plexiglas impressions from both 200 μ in. and 2800 μ in. Armco Iron surfaces.

It is quite generally agreed that for common machining and finishing operations, the wavelength of both roughness and waviness irregularities is greater than the amplitude, often by more than an order of magnitude. Indicative characteristics are summarized in Table IV.

TABLE IV

SURFACE ROUGHNESS CHARACTERISTICS (106)

Specimen	Surface Preparation	Roughness (Arithmetic Av.) μ in.	Peak-Height μ in.	Roughness Wavelength μ in.
Beryllium	Hand Lapping	1.0	4.5	5500
Steel	Machine Lapped 3 μ diamond abrasive	0.9	5.8	700
Steel	Machine Lapped 20 μ diamond abrasive	13.3	81.5	700
Steel	Commercial Machine Lapp	1.9	8.4	600

Because of this general character observed with surfaces produced by a diversity of machining and finishing operations the void area normal to the direction of interfacial heat transfer is greater than the solid contact area, often over 99 percent of the total.

If an equation for the thermal contact conductance, h_c, is written in the form,

$$h_c = \frac{1}{R_c} = k \cdot L^n \qquad (24)$$

it will be recalled that the one contact model yields a value of n = 1/3 for elastic deformation and n = 1/2 for plastic deformation. However, when extending the analysis to the multiple contact case associated with practical interfaces different values of n may be obtained depending on the distribution of the total contact area between different types of contacts. Variation of this distribution as a function of load is, of course, related to surface roughness and waviness. The pitfalls in disregarding "higher order" surface irregularities (e.g. waviness) when applying a relationship such as Equation 24 have been discussed by Archard (Reference 107). In the case where surface waviness is important, the constriction resistance resulting from individual closely spaced contact may be negligible compared with the large constriction resistance of the general contact area. Archard points to experiments with crossed cylinders having rough surfaces, where the contact is poor, which give values of contact conductance agreeing well with theoretical values based on smooth contact members. If surface films are present and their thermal conductivity is low, the overall constriction becomes area dependent rather than radius dependent (Equation 2a); in turn, the single contact exponent in Equation 24 is doubled.

For any model which assumes that increasing load gives an increase in both number and size of the contacts, the exponent in Equation 24 will be higher than the single contact case. Experimental measurements of Holm (Reference 86) and Bowden and Tabor (Reference 93) and analytical studies of Ling (Reference 108) confirm this.

If an interface is made up of surfaces which have been especially prepared with macroscopic irregularities such as pyramids (Refererence 57), unidirectional ruling (Reference 90) or spherical curvatures (Reference 88), it is possible to write a relatively simple geometrical equation for the contact area and void dimension as a function of relative surface orientation and to write approximate expressions for the variation of these quantities with compressive load. For surfaces developed through more conventional means in which both microscopic and macroscopic roughness patterns are formed, the surface characterization in terms of simple parameters becomes difficult. The following approaches which can be applied for roughness and/or waviness description have been suggested:

1. Direct Numerical Integration Analysis

2. Derivative Analysis

3. Statistical Analysis

Direct numerical integration of true surface profile data has been used successfully in estimating solid-solid contact area, A_s, average void thickness, δ , and the number of contacts per unit area, n. To simulate the effect of compressive loading Fenech (Reference 57) displaced superpositioned profiles of the contacting surfaces such that they overlapped to varying degrees. This was done with two profiles from both contacting surfaces taken perpendicular to each other. Equations of the following form were thus developed,

$$\frac{A_s}{A_T} = \frac{\sum_{i=1}^{n} \sum_{j=1}^{m} a_i\, b_j}{l_x\, l_y} \tag{25a}$$

$$n = \frac{n_x\, n_y}{l_x\, l_y} \tag{25b}$$

where,

a_i = width of the i^{th} contact between two superimposed profiles taken along the "x" direction

b_i = width of the i^{th} contact between two superimposed profiles taken perpendicular to "x" along "y" direction

l_x, l_y = total length of the recorded profiles

n = number of contacts between the superimposed profiles

The major difficulty associated with the above technique is the great amount of effort involved in surface profile analysis. In order to simplify the procedure, Henry (Reference 58) developed an analog computer program which could handle the calculations. The results from random lay, stainless steel surfaces, prepared by blasting with glass spheres, are presented in Table V. One specimen had an RMS roughness of 62 μ in., the other of 150 μ in. Comparison of analog computations on glass-blasted surfaces with direct determination of the number of contact per unit area through radioactive counting techniques showed excellent agreement.

TABLE V

CHARACTERISTICS OF RANDOM LAY FINISH,
STAINLESS STEEL CONTACT (Reference 58)

Load, psi	$\delta\mu$ in.	A_s/A_{total}	$(A_s/A)/n$, mils^2
1750	322	0.005	2.37
3460	305	0.01	3.31
6860	282	0.02	4.20
10200	261	0.03	4.75
17000	228	0.05	5.33

A second method of surface profile analysis which could be employed when the roughness patterns are of a fairly regular nature is described by Meyers (Reference 109), according to the following equations:

$$S_1 = \text{standard rms roughness} = \frac{1}{L}\sqrt{\int_0^L y^2\,dy} \qquad (26a)$$

$$S_2 = \text{1st derivative} = \frac{1}{L}\sqrt{\int_0^L \left(\frac{dy}{dx}\right)^2 dx} \qquad (26b)$$

$$S_3 = \text{2 nd derivative} = \frac{1}{L}\sqrt{\int_0^L \left(\frac{d^2y}{dx^2}\right)^2 dx} \qquad (26c)$$

These parameters are of no direct use in analyses requiring explicit definition of surface irregularity dimensions. However, for some types of contacts with more or less regular surface undulations, the parameters S_2 or S_3 may be a sensitive index of contact resistance variations. It is clear that the S_2 parameter would be particularly effective index for correlating reflectance characteristics of roughened surfaces. For two surfaces in contact, the number of contact points per unit length of profile would be the number of times a positive slope is encountered in moving along the profile at some reference height corresponding to the surface mean. Meyers indicates that the parameters S_1, S_2, and S_3 were computed by analog techniques in studies of surface friction characteristics. As would be expected, the first derivative parameter, S_2 was the most sensitive index of variations in sliding contact measurements.

For surface finishes which are nearly random in nature a third method of surface characterization may be useful. The method is based on the fact that in many cases surface irregularities may have nearly a Gaussian distribution. If this condition is met, only one parameter, the standard deviation, σ, is required to specify the distribution of surface irregularities. If two such surfaces are brought together

the distribution of their sum is also Gaussian. If Z_1, and Z_2 are the heights of the two surface profiles above their respective means and if the profile means are separated by a distance Z, the probability per unit length that the profiles will overlap is given by the probability that $Z_1 + Z_2 > Z$. Thus

$$\epsilon = p(Z_1 + Z_2 > Z) = \int_Z^\infty \frac{e^{-(Z_1+Z_2)/2\sigma^2_{Z_1+Z_2}}}{\sqrt{2\pi}\ \sigma_{Z_1+Z_2}} \qquad (27)$$

The integral is a tabulated probability function. The separation Z is the average void thickness δ. The number of solid-solid contacts per unit profile length is obtained by finding the standard deviation of the profile slopes.

The assumption of normal distribution was verified by Henry (Reference 60) on glass-sphere blasted stainless steel surfaces. Calculation of thermal contact conductance values based on this random process theory were in fair agreement with experimental results.

The degree of applicability of the above surface characterization methods in contact resistance correlation is dependent to a great extent on the types of finishes encountered and on the order of surface irregularity which is predominant. In addition, for the derivative and statistical approaches no correction is included for change in asperity geometry with load. Incorporation of such a factor is difficult since complex elastic-plastic deformations must be converted to explicit geometrical correction factors.

D. VOID PHASE CONDUCTION

As discussed connection with Equations 6 and 16, the void conduction contribution is usually estimated from some function of the void phase conductivity divided by an effective or average void thickness. In some cases it is assumed that radiation contributions are included in an effective gaseous conductance (Reference 57). Implicit in the definition of an effective gap width, δ, is the assumption that the heat flow through the gaps is along parallel lines and hence that this resistance is independent of the shapes of the irregularities (Reference 97). As discussed earlier this condition was incorporated in the expression developed by Fenech and Rohsenow. By direct analysis of profilometer traces Henry (Reference 60) obtained values of $\delta = 300\,\mu$ in. for sandblasted surfaces with RMS roughness values around 50 μ in. The more widely used approach is to estimate void conduction contributions by varying the gaseous environment or by calculating the difference between total contact conductance and the estimated solid-contact conductance. Sanderson (Reference 61) found for smooth (10 μ in. CLA) uranium-magnesium alloy interfaces that $h_{helium} > h_{argon} > h_{vacuum}$. The difference steadily decreased with increased compressive load, however, so that at higher loads about 80 percent of the conduction is across the solid-solid contacts. Somewhat contradictory results concerning the importance of the gaseous conduction component are reported by Held who maintains that even at loads up to 500-600 psi on steel and aluminum surfaces gaseous conduction is overwhelmingly important (Reference 110). On varying the gas pressure Sanderson observed that below 5 torr gas conduction was approximately zero in all cases. A similar limit for gas conduction contributions was observed by Shlykov and Ganin (References 111, and 112) and by Boeschoten and van der Held (Reference 67).

In the Russian work of Dyban and Shvets (References 27, and 113) it was concluded that gaseous conduction was overwhelmingly important at all load levels. Based on more or less qualitative analysis of extensive contact resistance data for steel, copper, brass and aluminum alloy interfaces these authors maintain that the decrease of the interfacial resistance with increasing load is due mainly to a reduction in the effective thickness of the gas film rather than to increased solid-solid contact area. Further, at higher compressive loads it is maintained that the thermal resistance of the contact decreases with increasing temperature level as a result of increased gas phase thermal conductivity rather than to decreased metal hardness. Similar conclusions are drawn by Sonokama in tests at moderate loads (Reference 114). In order to better understand these apparent contradictions, the results of Dyban and Shvets and the results of Sanderson (Reference 61) for different gaseous environments are compared in Figure 10.

To sketch the plots on the same basis and to eliminate effects due to variable test temperature and test material the independent coordinate chosen is the applied load divided by the hardness at temperature. From Equation 19 this variable is seen to be proportional to the solid-solid contact area. The comparison helps to explain, in at least a qualitative sense, the differences in conclusions drawn by the investigators. It also illustrates the fact that generalized conclusions based on limited testing are often more misleading than they are useful. Even though compressive loads up to 5600 psi were used in the Russian work as compared to a maximum load of 285 psi used by Sanderson, the solid-solid contact areas are comparable. The fact that the roughness levels are different is highly significant even though L/H ranges are similar. The constriction resistance is substantially higher for the rougher surfaces studied by Shvets and Dyban and it is seen from Figure 10 that this condition masks effects of the higher aluminum alloy conductivity which would tend to increase the solid conduction contribution. Here gas conduction is clearly important at all load levls whereas Sanderson's results show that the gas conduction contributions were eliminated at L/H values between 0.04 and 0.05. Further it is clear that the relative proportion of gas phase conduction is different in these two sets of curves and changes in dissimilar fashions with increase in load. The differences in both constriction resistance and thermal conductivity of the contacting members influence the nature of the net variation in overall contact resistance with load. Thus the conclusions of these investigators regarding gas conduction contributions are really not contradictory. Effects of higher order surface irregularities (e.g. waviness) could produce essentially the same results. However, these authors did not provide sufficient surface characterization data to allow further analysis.

Finally there are several additional factors which should be kept in mind in assessing void phase conduction contributions. First, the effective gaseous conductivity becomes a function of the gap geometry when the molecular mean free path, λ, becomes comparable to the effective gap width, δ. This situation could exist at atmospheric pressure when $\delta \cong \lambda$, depending on what gas is present. Of course, as the gas pressure is reduced this condition will be reached eventually for any value of δ. Second, the exchange of energy between the gas and solid at their interface may be highly inefficient as reflected in accommodation coefficients considerably less than unity. In this case a correction may be applied to Equation 6 by increasing δ to account for this effect as suggested by Robertson et. al. (Reference 62). Expressions for effective gas conductivities as a function of temperature pressure and accommodation coefficient are developed in standard texts and will not be considered further except to indicate that accurate estimation of accommodation coefficients for real surfaces is extremely difficult. Further discussion of these effects will be included in Section V.

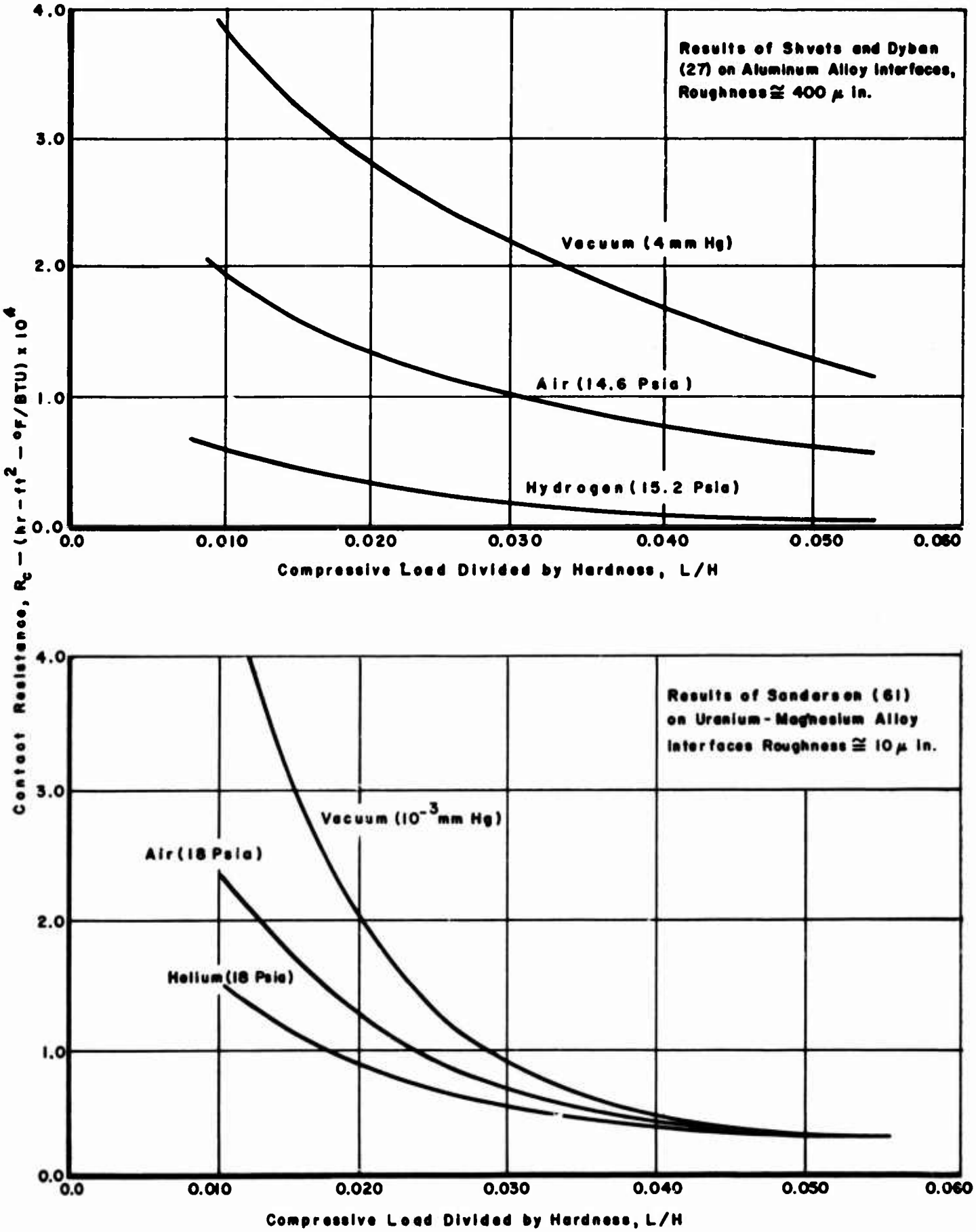

Figure 10. Thermal Contact Resistance as a Function of Load in Different Gaseous Environments

The final general observation relating to gas conduction effects concerns the widely used approximation that the total thermal contact conductance is equal to the sum of the solid-solid conduction and the effective void conduction where the solid conduction contribution is established through the measurements in vacuum environment. For the physical situation encountered across an interface, superposition of the heat flows is only a valid approximation when one of the components is highly predominate. Thus, in cases where there is an apparent transition from heat flow predominantly across the void area to heat flow predominantly across the solid contacts, it is highly unlikely that the simple superposition approach is applicable. It is difficult to attempt quantitative assessment of void phase conduction contributions by varying gas thermal conductivity while assuming a constant solid-solid conduction component since significant redistributions of the heat flux between the solid and gas paths may be occurring.

SECTION V

EXPERIMENTAL-ANALYTICAL CORRELATIONS

A. CORRELATIONS BASED ON LIMITED DATA

To conclude this review a brief discussion is made of those investigations in which a successful correlation has been affected between analytical predictions and experimental results. In early studies during the 40's, surface characterization was generally limited to the determination of the arithmetic or RMS roughness. These values were used in either qualitative or empirical correlations of contact resistance variations as a function of applied load (References 114, 115, 116).

The first analytical study of any depth was that of Cetinkale and Fishenden (Reference 87) who expanded on the one-contact model to include effects of gas conduction across the void area. The expressions for the solid and gaseous conduction components given in Equations 5b and 6 were combined as in Equation 28 below,

$$h_{total} = \frac{1}{R_{total}} = \frac{1}{R_g} + \frac{1}{R_s} = \frac{\pi b^2 k_f}{\delta} + \frac{2\pi a k_s}{\tan^{-1}\left[\frac{(X_d - a)}{a}\right]} \qquad (28)$$

The final equation for h_{total} was converted to dimensionless form to establish the general functional dependence of the contact conductance on three dimensionless groups: the constriction number, $C = a/b$, the conductivity number $K = k_g/k_s$ and the fluid thickness number, $B = \delta/b$. The dimensionless conductance number, $U = h_T \delta/k_g$ was then given by the following expression,

$$u = h_T \frac{\delta}{k_g} = 1 + \frac{BC}{k \tan^{-1}\left\{\frac{1}{C}\sqrt{(1 - \frac{1}{u})-1}\right\}} \qquad (29)$$

These groups were written in terms of empirical factors which were evaluated for a series of very rough (8,000 to 34,000 μ in. peak-to-peak) metallic interfaces. Although none of the experimental contact resistance data was presented, it was stated that the empirical correlation was successful for steel, aluminum and brass interfaces with air, spindle oil and glycerol as the interfacial fluid.

Using a relationship similar to Equation 22 in estimating the solid-solid conduction area from hardness data and assuming that the gaseous conduction component is proportional to the ratio of the effective gap width to the gas conductivity, Tachibana (Reference 97) expressed the overall thermal contact conductance as the sum of the solid and gas phase components. The equivalent thickness notation was used, one being equal to R_c times an effective thermal conductivity. The final relationship is given by Equation 30.

$$\frac{1}{\ell} = \left(\frac{1}{Y + Y_c}\right)\frac{P}{CH} + \frac{1}{Y}\,\frac{k_g}{k_s} \qquad (30)$$

The effective mean height of the surface irregularities, y, was found to be constant for a given type of surface machining operation; the factor, y_c, is a small correction to y accounting for minute irregularities across the areas of direct contact. A generally linear relationship was found experimentally between $\frac{1}{\ell}$ and P thus

confirming the validity of Equation 30. The values of C and y were determined from data obtained with surfaces having variable finishes. The empirical deformation factor, C, (ξ in Equation 22) assumes a value of 2.5 in order to correlate the data. The contact resistance measurements were made with gun metal specimens of three peak-to-peak roughnesses: 140, 600 and 1200 microinches. Parafin, oil and air were used as void phase materials. Even though it was concluded that the single surface finish parameter y was sufficient to provide a correlation, the experimental verification of this simple contact conductance equation can only be considered as qualitative, however, since only limited data on very rough specimens was obtained.

Starting with the one contact model, Held (Reference 110) used the classical Hertz equations for elastic deformation to write a simple equation for the resistance of one contact as a function of load. Based on the elastic deformation equations an expression was also written for the "degree of flattening", u; this parameter is the amount by which the surfaces approach each other as a function of load. Even for the elastic deformation case, to extend the one contact equation to the true multiple contact interface encountered in practice it was necessary to establish a relationship between the load (or u in this analysis) and the number of contacts, n. Assuming no interaction between adjacent contacts Held employs an equation of the form

$$n = f(u) = Mu^{M} \tag{31}$$

where,

M, m = empirical constants

The final expression for the contact conductance of an interface where the asperities are being elastically deformed, is then in terms of m, M, u, r - the average radius of curvature of the asperities, and the material properties. The radius of curvature, r, is estimated from profilometer traces of the surfaces.

$$h_{elastic} = 2k\alpha^{\frac{2m+1}{2m+3}} \beta\left(M\sqrt{r}\right)^{\frac{2}{2m+3}} L^{\frac{2m+1}{2m+3}} \tag{32}$$

where,

$\alpha = 1.5(1-\mu^2)/E$, (μ = Poisson ratio, E = elastic modulus)

β = constant = f(m)

r = asperity radius of curvature

M,m = constants defined by Equation 31

L = load

The same approach was employed for the plastic deformation range by defining the plastic deformation analogy of Equation 31 in terms of the two constants M^1 and m^1. For this case it is assumed that the true area of contact is equal to the load divided by the Brinnell hardness. Since the thermal contact conductance equations derived in this manner are of the form,

$$h_c = BL^{\beta} \tag{33}$$

β, B = constants ($1/3 \le \beta \le 1$: elastic deformation; $1/2 \le \beta \le 1$: plastic deformation)

the experimental results of contact conductance, h_c, as a function of load, L, in air environment were plotted on log-log coordinates. Seven different degrees of roughness on steel specimens were developed ranging from polished and lapped to coarsely lathed interfaces although no quantitative description of the various surfaces was given. Both compression and decompression cycles were run, a substantial hysteresis being observed for all ranges of surface roughness. The fact that the log-log plots of contact conductance as a function of load gave straight-line curves at loads up to 3800 psi with slopes between 0.5 and 1.0, was said to confirm the validity of the principles upon which the theory is based. No further analysis is given beyond establishing the range of the exponent in Equation 33.

Starting with Equation 28, Shlykov, Ganin and Demkin (References 111, and 112) attempted to establish a simple relationship between the compressive load, the mean gap width, δ , and the solid-solid area of contact. Through analysis of surface profile traces on steel specimens it was concluded that the simple relationship given in Equation 34 was sufficient to geometrically characterize the surface under load.

$$\epsilon = \frac{A_s}{A_T} = b\left(\frac{\delta_{max} - \delta}{\delta_{max}}\right)^d \tag{34}$$

where,

δ_{max} = maximum height of the asperities

δ = mean gap width which is a function of load

b,d = empirical constants

For lathe turned and milled surfaces d = 2 and b = 2-3; for ground surfaces d = 3 and b = 5; for buffed surfaces d = 3 and b = 10-15. The experimental results indicated that the "relative approach", $((\delta_{max} - \delta)/\delta_{max})$, did not exceed 0.1 for the steel surfaces considered. On the basis of this observation the gas conduction contribution was calculated using δ_{max}, the corrections in terms of d and b being neglected, i.e., Rg = $\delta max/k_g$. The solid conduction component was derived from Equation 34 employing the assumption that the size of the contact spots remained essentially unchanged during compression, and that the enlargement of the actual field of contact occurs primarily because of the increase in the number of contacts. This assumption together with an assumed asperity radius of 30 μ was based on the experimental observations of Holm (Reference 86), Shvetzova (Reference 105) and Boeschoten and van der Held (Reference 67). The extent of elastic deformation as a function of the relative approach was estimated from the Hertz equations. Plastic deformation was assumed to be fully initiated when the contact stress (hardness) equalled 3Y, where Y is the yield limit of the work hardened material. With the above assumptions the solid conduction contribution was calculated using Equation 2b

$$\frac{1}{R_s} = 2\,a\,n\,k_s \tag{2b}$$

where,

a = average radius of solid-solid contact = 30 μ

n = number of contact spots per unit area,

$$n = \left(\frac{1}{\pi a^2}\right)\frac{A_s}{A_T} = \frac{1}{\pi a^2}\left[f(b, d, Y, L)\right]$$

The results of the full deviation are given in Equation 35.

$$\frac{1}{R_T} = \frac{1}{R_g} + \frac{1}{R_s} = \frac{2K_g}{\delta_{max}\left[1 - \frac{p}{Hb}\right]^{1/d}} + \frac{2K_s}{\pi a}\left[\frac{p}{H} + \frac{d}{2}\epsilon b^{1/d}\left(\frac{p}{H}\right)\frac{d-1}{d}\right] \qquad (35)$$

Extensive further simplifications were made in Equation 35 before comparison with experimental results by assuming that elastic deformation contributions were small and that A_s/A_T is simply the ratio of the compressive force to the material hardness. On this basis the second terms in the right-hand bracket, Equation 35 was eliminated. The final result used, for comparison with the experimental results was then quite simple, as shown in Equation 35a,

$$\frac{1}{R_T} = \frac{2k_g}{\delta_{max}} + Ck_s\left(\frac{p}{H}\right) \qquad (35a)$$

where,

C = constant

Experimental data on contact conductance as a function of load was presented for stainless steel specimens ranging in roughness from about 40 μ in. to 400 μ in. (4th to 9th class finishes). In general the agreement between the data and the simplified analytical equation, Equation 35a was within about 20 percent. At loads above 1500 psi the deviations for rough finish contacts were attributed to increase in the solid-solid contact area due to flattening of the asperities which was not accounted for in the equations used. It is interesting to note that because the relative approach of the steel interface members was limited to about 0.1, these authors conclude that the reduction in contact resistance with load is due to the enlarged solid-solid contact area rather than to a reduced gas-layer thickness. On the other hand the Russian work of Dyban and Shvets (References 30, 31) on steel specimens with similar finishes showed that reduction in gas layer thickness was of great importance in reducing the overall contact resistance.

The derivation of the contact conductance equation obtained in the boundary value solution for the one contact model with void-phase conduction was discussed in connection with Equation 16. In this contact conductance equation, developed by Fenech and Rohsenow (Reference 57), the physical variables n, A_C/A_T and δ were obtained by matching the profilometer traces obtained on the contacting surfaces. Experimental verification of the analytical results was first attempted with a single contact cylinder (Figure 3a) using air, water and mercury in the annular groove. The results of these tests were successfully correlated with predictions. Contact conductance tests on an interface made up of roughly milled Armco iron ($\sim 100\,\mu$ in. RMS) and aluminum ($\sim 50\,\mu$ in. RMS) were completed to check validity of the theory for a more practical interface. The experimental results here agreed with the predicted conductance values within about 5 percent over a load range from 100 to 2600 psi. The large hysteresis observed on cycling of the compressive load for the iron-aluminum contact could not be accounted for quantitatively since elastic deformation was not included in the analysis; nor was the effect of plastic flow along the asperity surfaces considered. Further work based on the equations formulated by

Fenech was carried out by Henry (Reference 58) who developed an analog computer technique for evaluation of the surface profile parameters, m, Ac/At, and δ . The computer input was in the form of analog voltage traces of the surface profiles on magnetic tape. Two recorded profiles were fed simultaneously in the computer to allow calculation of the interface contact parameters. Experimental tests were conducted on an interface consisting of two stainless steel specimens with roughness of 62 and 150 μ in. RMS. Blasting with glass spheres produced a specimen surface finish with random lay. Thermal contact conductance data as a function of compressive load from 300 to 20,000 psi were obtained at three mean in interface temperatures: 100°, 200° and 350°F. The comparison between analytical predictions and experimental results were plotted as log h_c vs log P so that it is difficult to accurately estimate agreement. It was stated that the maximum deviation of predicted values from the experimental data was 30 percent, occurring at the higher loads. Experimental accuracy is of course reduced at high loads because the interfacial temperature drops are very low. The author reported values on the order of 1 to 3°F at 20,000 psi.

The problem of surface characterization can add substantial complexities to even semi-empirical analyses of contact conductance as indicated in the above paragraphs. In attempting to avoid this problem Laming (Reference 90) used contacting members which had regularly machined patterns in the form of parallel grooves, cut with a fine, single point tool. The resulting finishes were fairly rough, with peak-to-mean distances ranging from 170 to 2000 μin. The wavelength of the grooves averaged approximately 10 times the peak-to-mean distance. Following the same line of reasoning used in arriving at Equation 20, the following expression was developed for the total contact conductance, h_c.

$$h_c = \frac{k_f}{\delta} + \frac{2k_s}{(1-f)} \left[\frac{\sin \alpha}{\pi \lambda_1 \lambda_2} \cdot \frac{L}{H_M} \right]^{\frac{1}{2}} \qquad (36)$$

The first term in the bracket gives the number of solid-solid contacts per unit area for ruled surfaces having wavelengths λ_1, and λ_2 and which are oriented at a relative angle α . The term $(1/1-f)$ accounts for constriction alleviation at high loads (cf Equation 10). Laming assumed that the gaseous conduction component as a given by the first term of Equation 36 was load independent. Since f and H_m in the solid conduction term of this equation are load dependent, the author assumed that the entire term was a simple exponential function of the load. Log-log plots of the experimental contact conductance data as function of load were prepared followed by the determination of a constant (representing k_f/δ) which, when substracted from h_c, resulted in a straight line on the plot. Determination of the gas conduction component by this method gave results which agreed favorably with direct experimental data on the gaseous conduction components obtained by varying the interfacial fluid at constant load. The equivalent film thickness was found to be $\delta = 2/3\,\zeta$ where ζ is the peak-to-mean distance.

Observed deficiencies in the use of Equation 36 were: 1) conductances were not as high as predicted, 2) a slope > 0.5 was found for the log-log conductance vs load plots, and 3) conductance values for interfaces with fine finishes had proportionately lower conductances than the coarse-finish interfaces. Increased apparent hardness of the finer contact points was said to account for most of these effects.

Using Equation 36 with empirically determined constriction alleviation factor and load dependent hardness, good correlation was obtained for contacts made up of brass, steel and aluminum surfaces with both similar and dissimilar peak-to-mean roughnesses.

The fact that contacting surfaces undoubtedly have some degree of waviness or surface undulation on a macroscopic scale in addition to the more commonly studied microscopic roughness has been recognized as discussed earlier. Clausing and Chao (Reference 88) pointed out that neglect of waviness effects have raised serious reservations about the conclusions drawn by other investigators considering only microscopic roughness contributions. Thus in the results of Boeschoten and van der Held discussed earlier (Reference 67) the relatively large contact area diameter (60 μ) appeared to be inconsistent with the low surface roughness values (around 10 μ in.); the inconsistency is attributed to neglect of surface waviness by Clausing and Chao. Other investigators have used the value of 60 μ for nominal contact point diameters in developing their correlations as discussed earlier. In the analysis by Laming (Reference 90) where the same type of analytical contact conductance equation was used, a very high value of surface hardness was required to correlate the experimental data. Clausing and Chao postulate that since the solid-solid contact conductance term included the macroscopic constriction resistance due to waviness, the extremely high hardness value is a natural consequence of neglecting this contribution.

In their experimental-analytical correlation work, Clausing and Chao considered only macroscopic resistance or waviness effects, beginning their analytical development with Equation 11. Assuming that the macroscopic constriction region was established through elastic deformation only, the contact area or more properly the parameter $x = a/b$ can be written as a function at the waviness amplitude. In dimensionless form this deformation parameter was defined as the elastic conformity modulus, ξ ,

$$\xi = \left(\frac{L}{E}\right)\left(\frac{a_M}{d}\right) \qquad (37)$$

where,

a_m = radius of macroscopic construction region (Figure 1a)

d = equivalent flatness deviation

(d $\cong$ waviness amplitude)

ξ is the ratio of the elastic deformation to the flatness deviation and is a measure on a macroscopic scale of the degree of conformity of the mating surfaces. Writing the dimensionless macroscopic contact conductance in Biot modulus form where $X = a/b$ Equation 11 becomes,

$$\frac{h a_M}{k_s} = \frac{2X}{\pi g(x)} = f(\xi) \qquad (38)$$

Experimental investigations to check the analytical predictions were limited to very smooth surfaces (3μ in. roughness) where only macroscopic construction resistances would be anticipated. Surface waviness characterization was accomplished by optical interference pattern analysis. This technique, of course, is limited to surfaces with very low roughness - on the order of 10 μ in. or less. After polishing it was generally observed that the surfaces of the brass, aluminum, stainless steel and magnesium specimen were nearly spherical. Fairly good agreement between predicted and measured contact conductances was found for all test materials when the Biot modulus was plotted as a fraction of the elastic conformity modulus. Relatively poor correlation in the case of aluminum was attributed to oxide film formation.

Hysteresis in the contact conductance on load cycling was observed. This effect was not included in the initial derivation based on purely elastic deformation. The dimensionless parameter correlation, however, seemed somewhat insensitive to such deviations.

The correlations discussed in this section have been based on experimental results which are generally very limited usually those obtained by the author. Even under these circumstances, many of the developments were semi-empirical. Comparisons of experimental results among different investigators have not been outstandingly successful for reasons which should now be apparent. Two efforts along these lines deserve mention however and are discussed in the last section of this review.

B. GENERALIZED CORRELATIONS

Recalling the discussion in Section IV-D on Void Phase Conduction, it was pointed out that imperfect transfer of energy from gas to solid could reduce the net gas phase conduction and thus increases the effective gap width. This phenomena was considered in some detail by Rapier, Jones and McIntosh in the course of a study on gas conduction contribution to the contact conductance (Reference 63). In their work with uranium dioxide-stainless steel interfaces, the solid conduction contribution was low in all cases due to the hardness of the contacting members and the low conductivity of the uranium dioxide. The experimental values obtained for the solid conductance were of the same order as that predicted by Centinkale and Fishenden (Reference 87) using Equations 5a-5b. The gas phase contribution was studied extensively since for the reactor applications where canned UO_2 fuel elements are used, a low overall interfacial resistance could be achieved by increasing the gas phase conduction.

The increase in the effective interfacial gap width distance due to the gas-solid accommodation effect was expressed in terms of an accommodation coefficient jump distance, g, derived from kinetic theory, Equation 118,

$$g = \lambda \left[\frac{2}{N_{Pr}} \left(\frac{2 - \alpha}{\alpha} \right) \left(\frac{\gamma}{\gamma - 1} \right) \right] \tag{39}$$

where,

λ = mean free path of the gas molecules

N_{Pr} = Prandtl Number

α = accommodation coefficient

γ = specific heat ratio

Several expressions were developed for the effective gap width including this contribution assuming a number of idealized surface geometries. The parabolic

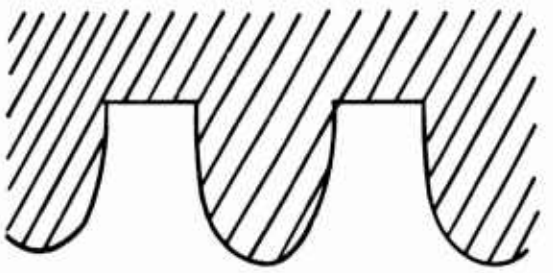

profile indicated on the preceding page was used to define a surface having gaps with radial symmetry about the contact points. The result of the integration gives the following expression for a dimensionless gap width parameter, Y, in terms of a dimensionless accommodation coefficient factor, X.

$$Y = \frac{0.6}{(1 + 0.5X)} + 0.4 \ln(1 + 2X) \qquad (40)$$

where,

$Y = \delta_{max} / \delta_{eff}$

$X = \delta_{max} / 2g$

$\delta_{max} = \delta_1 + \delta_2$ = maximum gap width of two surfaces in contact having paraboloid asperities.

δ_{eff} = effective "volumetric" mean gap width

In Equation 40 the 'X' term coefficients were arbitrarily multiplied by a factor of 2.0 in order to yield good agreement with the experimental data obtained by these authors. No quantitative explanations were offered for the fact that the measured X values were low by a factor of two, however, the following effects were cited as contributing causes:

(1) Uncertainties, particularly overestimates, in the jump distance, g.

(2) Underestimates of δ_{max} due to difficulties encountered in surface profile definition.

An extensive number of experimental contact conductance measurements with the UO_2-stainless steel interfaces were made in vacuum and various inert gases to establish the generality of Equation 40. The effective gap width was determined from Equation 41,

$$\delta = \frac{k_f}{h_f} = \frac{k_f}{h_T - h_s} \qquad (41)$$

where the solid contact, h_s, was obtained from vacuum environment measurements. The g values for helium, neon and argon were calculated from Equation 39 using accommodation coefficient data from the International Critical Tables. In a plot of X as a function of Y over the range 0.1 X 50, all the data points obtained by the authors fell along the curve defined by Equation 40.

Comparisons were then prepared between predicted gas conduction values given by Equation 40 and the experimental results of other investigators. The overall results are given in Figure 11 including the data of these authors. Considering the wide variety of test materials, measurement methods and interface gases which these data points represent, the agreement is quite good. In particular Rapier, Jones and McIntosh have obtained extensive data in the region where the accommodation coefficient jump is comparable to or greater than the geometrical gap width ($X \leq 1.0$).

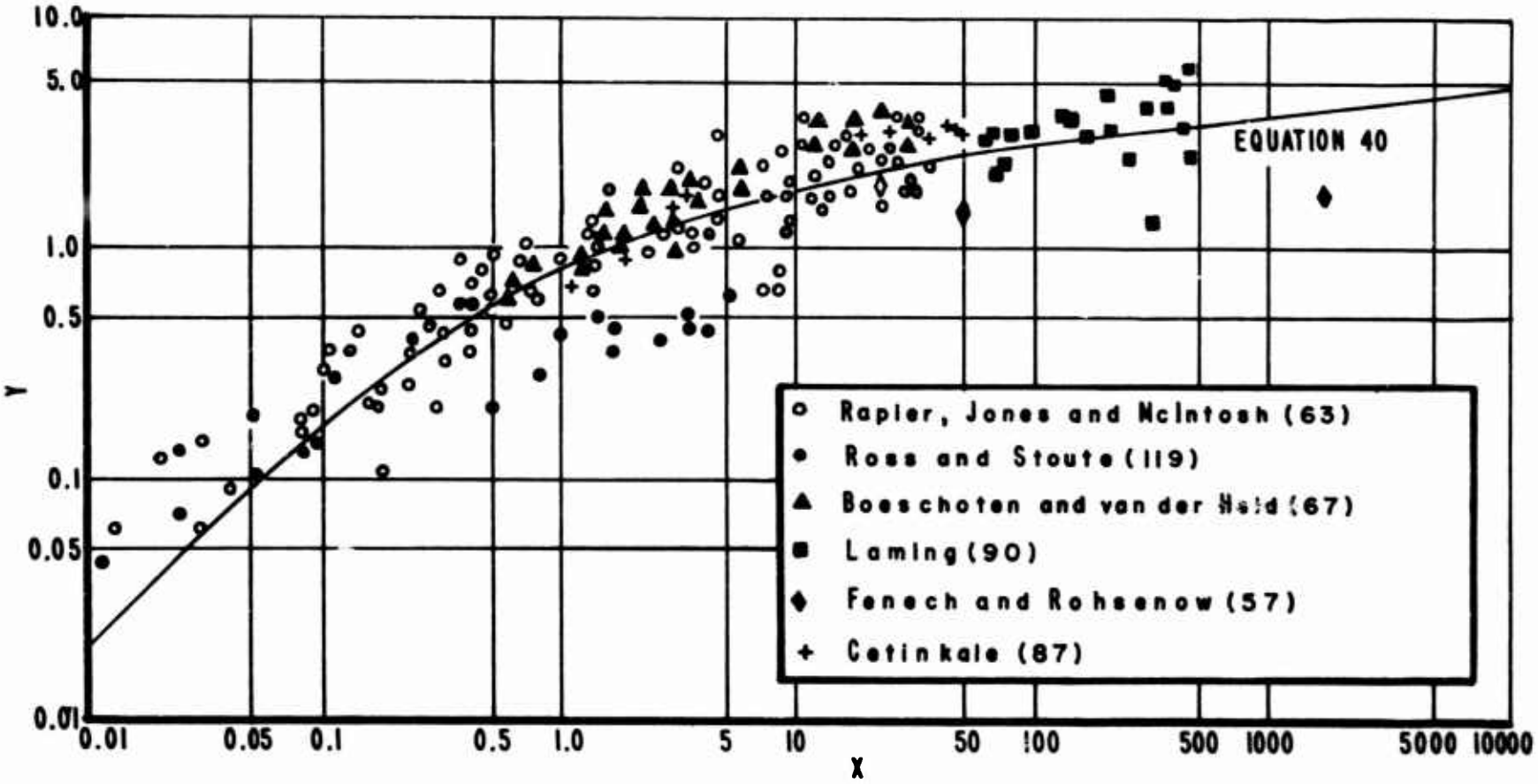

Figure 11. General Correlation of Gaseous Conduction Contributions to the Interface Conductance (Reference 63)

The variables X and Y have characteristics which tend to minimize scatter of the experimental data about the plot of Equation 40, particularly on a log-log representation. The equation is somewhat insensitive to surface profile variations since the factor δ_{max} appears as a coefficient of both the dependent and independent variables. Where X is large and Y is above unity the correlation is not really meaningful since the accommodation effects are small, the plot indicating only that for a given surface the geometrical relationship between δ_{max} and δ_{mean} is relatively independent of variations in δ_{max}.

It has been suggested by Graff (Reference 120) that generalized correlation of thermal contact resistance data can be affected by plotting the dimensionless conductance, $\bar{h}_c$ as a function of the dimensionless compressive pressure, $\bar{p}$. These parameters are defined by Equations 42a and 42b.

$$\bar{h}_c = \frac{h\rho}{k\rho} \tag{42a}$$

$$\bar{p} = \frac{p}{H} \tag{42b}$$

The success of this approach is indicated in Figures 12a and 12b where thermal conductance data from a number of literature sources are plotted for ferrous and nonferrous metals at mean interface temperatures between 70 and 200°F. Graff indicates that the spread of the curves in these figures is due mainly to variations in surface roughness. Data presentation in this form is clearly a convenient method of displaying results on a wide variety of materials having substantial variations in interface characteristics. Thus, the co-ordinates are suitable to the extent that it becomes possible to present a great amount of data in a single figure which is relatively easy to use in design applications. However, it is necessary to point out several characteristics of the plot which limit its significance as a true correlation procedure.

The appearance of the compressive force, P, in both the dependent and independent variables forces a superficial smoothing of the data and greatly decreases sensitivity of the plot to the several factors exerting an influence on the contact conductance. The independent variable P/H can be used with some physical justification since the ratio of the applied compressive force to the hardness is proportional to the area of direct contact (Equation 19a). Exactly what hardness value is used and whether it is load independent is difficult to decide as was discussed earlier in Section IV-B. Except for the pure elastic deformation case, where a parameter such as the elastic conformity modulus may be used, (Equation 37) it is reasonable to assume that the ratio R/H is proportional to the direct solid-solid contact area. It should be pointed out, though, that R/H values much greater than unity are difficult to rationalize physically.

For true data correlation it is doubtful that $\bar{h}_c$ as defined in Equation 42 is a valid dependent variable. Dividing through the coordinates of Figure 12 by the compressive force P and assuming that the quantity ρ x k is constant for a given material, it is found that the contact conductance is inversely proportional to the hardness of the contacting members and directly proportional to some power of the compressive force; based on the fact that the curves in Figures 12a and 12b have slopes greater than unity, this power is positive. This dependence is expected physically, however, if the dimensionless contact conductance, $\bar{p}$, is written in the form of the Biot modulus, $h\delta/k$, from Equation 41a, $\delta = P/\rho$. If the correlation were to be truly significant, the length term, δ, must be more directly related to

the effective gap width at the interface than the quantity P/ρ . As discussed in connection with Figure 10, the proper δ term can be most simply estimated from experimental measurements through the use of Equation 40. h_f is the conductance measured in vacuum and h_T is the value measured in a gaseous environment. Corrections to k_f for mean free path and accommodation coefficient effects were discussed earlier. A more extensive presentation of literature data using a similar approach was developed by Hsiech (Reference 123).

Curve	Type of Steel	Surface Roughness	Surface Condition	Ref.
1	1020	3	In Air	116
2	1020	32	In Air	
3	1020	85	In Air	
4	1020	1660	In Air	
5	1020	3320	In Air	
6	1020	3	In Argon	
7	1020	16	In Argon	
8	1020	55	In Argon	
9	1020	3320	In Argon	
10	1020	4	In Air	121
11	1020	63	In Air	
12	1020	63	In Air	
13	1020	125	In Air	
14	1020	125	In Air (Rusted)	
15	1020	1000	In Air	
16	1020m	1000	In Air	
17	1020	1000	In Air (Rusted)	
18	4140	100	In Air	117
19	4140	78	In Air	
20	AMS 5613	Extreme Roughness	In Air	57
21	416SS	30	In Air	13
22	416SS	100	In Air	

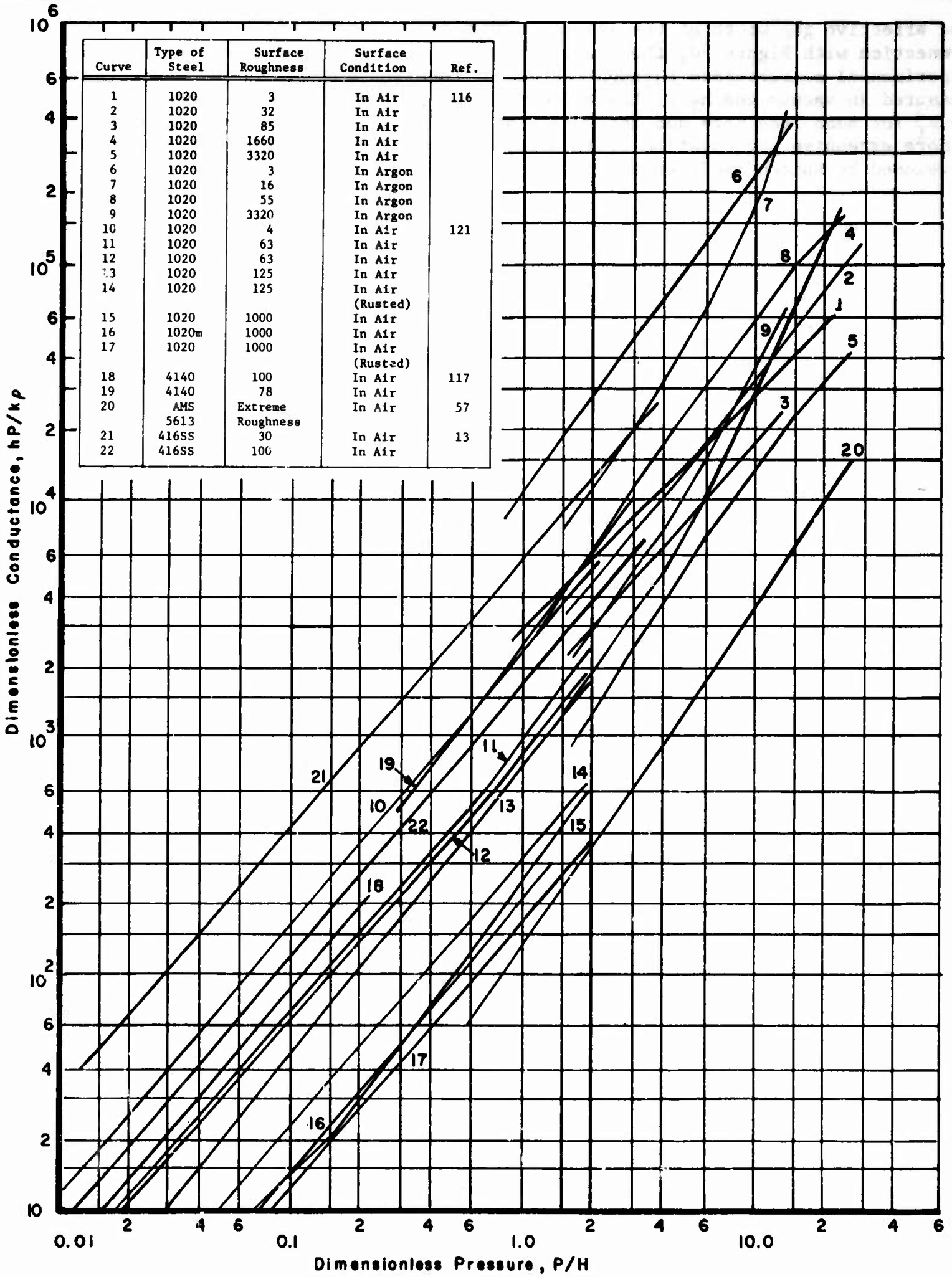

Figure 12a. Dimensionless Plot of Thermal Conductance versus Pressure-Ferrous Materials (Reference 120)

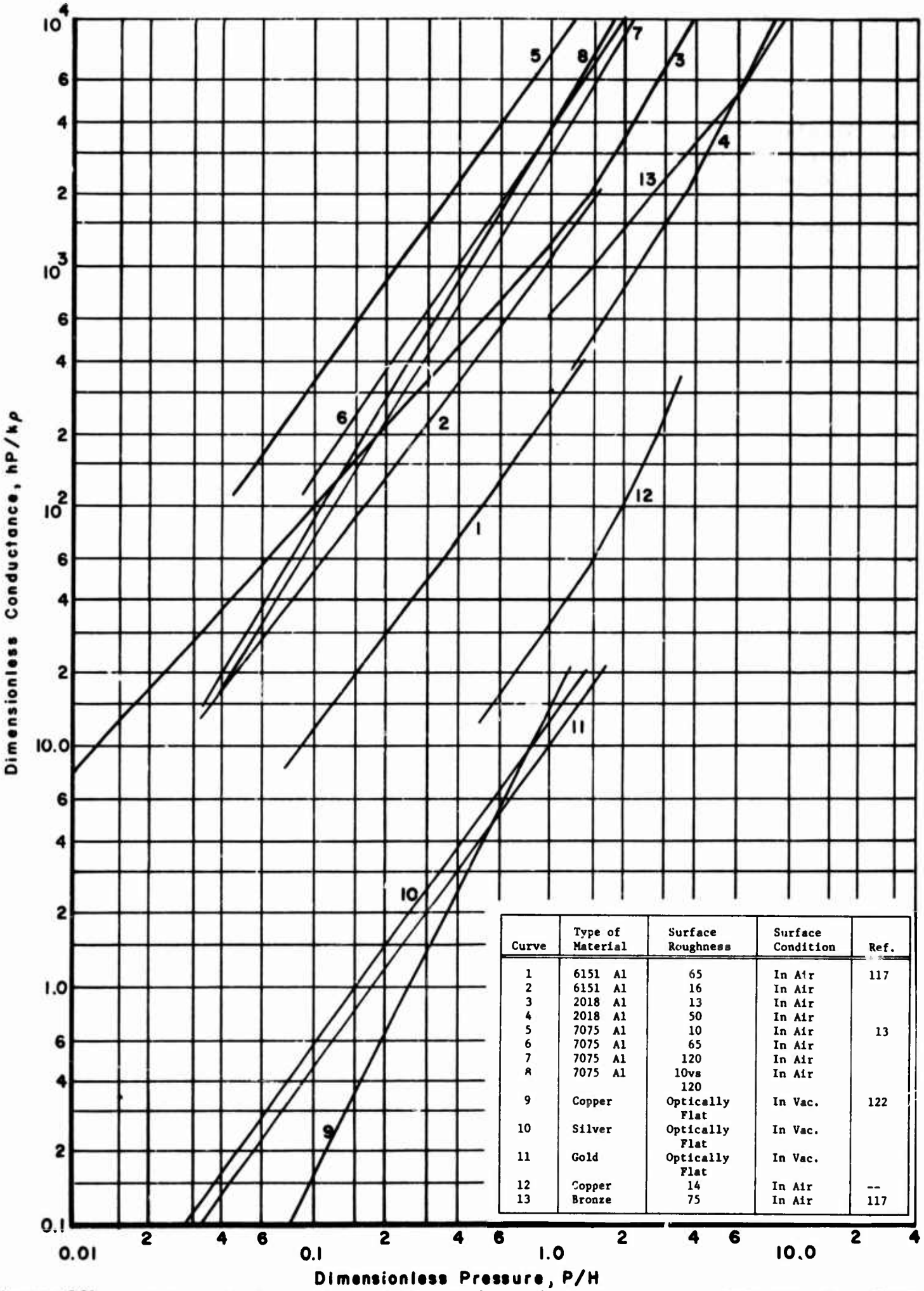

Curve	Type of Material	Surface Roughness	Surface Condition	Ref.
1	6151 Al	65	In Air	117
2	6151 Al	16	In Air	
3	2018 Al	13	In Air	
4	2018 Al	50	In Air	
5	7075 Al	10	In Air	13
6	7075 Al	65	In Air	
7	7075 Al	120	In Air	
8	7075 Al	10vs 120	In Air	
9	Copper	Optically Flat	In Vac.	122
10	Silver	Optically Flat	In Vac.	
11	Gold	Optically Flat	In Vac.	
12	Copper	14	In Air	--
13	Bronze	75	In Air	117

Figure 12b. Dimensionless Plot of Thermal Conductance versus Pressure-Non-Ferrous Materials (Reference 120)

SECTION VI

REFERENCES

1. Wheeler, R. G., "Thermal Contact Conductance", Hanford Laboratories Operation, General Electric Company, AEC Report No. HW-53598, (November 1957).

2. Wheeler, R. G., "Thermal Contact Conductance of Fuel Element Materials", Hanford Atomic Products Operation, General Electric Company, AEC Report No. HW-60343 (April 1959).

3. Robertson, J. A. L., Ross, A. M., Notley, M. J. F., MacEwan, J. R., "Temperature Distribution in UO_2 Fuel Elements", J. Nuc. Materials, 7, 225-262, (1962).

4. Henry, J. J., "Thermal Conductance of Metallic Surfaces in Contact", AEC Report No. NYO-9459, (February 1963).

5. Adamantiades, A., "Experimental Determination of Contact Conductance For Some Stainless Steel Contacts", AEC Report No. NYO-9458, (July 1962).

6. Fried, E., "Study of Interface Thermal Contact Conductance", General Electric, Summary Report, NASA Contract NAS 8-5207, (May 1964).

7. Cunnington, G. R., Jr., "Thermal Conductance of Filled Aluminum and Magnesium Joints in a Vacuum Environment", Lockheed Missiles and Space Co., (1964).

8. Coulbert, C. D., Liu, C., Thermal Resistance of Aircraft Structure Joints", WADC TN 53-50, (June 1953).

9. Wicken, G. W., (Translator), "Conductance Thermique Des Liaisons Der Tabs D'AU4GI", (December 1957), Royal Acft. Est. Trans. No. 949 (June 1961).

10. Wicken, G. W., (Translator), "Conductance Thermique des Liaisons Der Tabs D'AU4GI Collees", (March 1959), Royal Acft. Est. Trans. No. 952, (July 1961).

11. Brown, M. H. S., (Translator), "Conductance Thermique des Liasisons Acier", (March 1960), Royal Acft. Est. Trans. No. 950, (July 1961).

12. Barzelay, M. E., Tong, K. N., Holloway, G. F., "Thermal Conductance of Contact in Aircraft Joints", NACA TN 3167, (March 1954).

13. Barzelay, M. E., Tong, K. N., Holloway, G. F., "Effort of Pressure on the Thermal Conductance of Contact Joints", NACA TN 3295, (May 1955).

14. Barzelay, M. E., Holloway, G. F., "Effects of an Interface on Transient Temperature Distribution in Composite Aircraft Joints", NACA TN-3824, (April 1957).

15. Barzelay, M. E., Holloway, G. F., "Interface Conductance of Twenty-Seven Riveted Aircraft Joints", NACA TN-3991, (July 1957).

REFERENCES (Cont'd)

16. Barzelay, M. E., "Range of Interface Thermal Conductance for Aircraft Joints", NASA TN D-426, (May 1960).

17. Gatewood, B. E., "Effect of Thermal Resistance of Joints upon Thermal Stresses", Air Force Institute of Technology Report No. 56-6, (May 1956).

18. Lardner, T. J., "Thermal Joint Conductance: Midplane Stress Distribution", Jet Propulsion Laboratory Space Programs Summary No. 37-19, Vol IV, 83-85, (1963).

19. Lardner, T. J., "Effect of a Variable Thermal Joint Conductance", Jet Propulsion Laboratory Space Programs Summary No. 37-21, Vol IV., 53-56, (1963).

20. Aron, W., Colombo, G., "Controlling Factors of Thermal Conductance Across Bolted Joints in a Vacuum Environment", ASME Paper No. 63-WA-196, (November 1963).

21. Griffith, G. E., Miltonberger, G. H., "Some Effects of Joint Conductivity on the Temperature and Thermal Stresses in Aerodynamically Heated Skin-Stiffener Combinations", NACA TN-3699 (June 1956).

22. Griffith, G. E., Brooks, W. A., Jr., Strauss, H. K., "Two Factors Influencing Temperature Distributions and Thermal Stresses in Structures", NACA TN 4052, (June 1957).

23. Pohle, F. V., Lardner, T. J., French, F. W., "Temperature Distribution and Thermal Stresses in Structures with Contact Resistance", Air Force Office of Scientific Research, TN 60-504, (May 1960).

24. Barber, A. D., Weiner, J. H., Boley, B. A., J. Aero. Sci., 24, 24, 232-234 (1957).

25. Hines, W. S., "Experimental Study of Contact Resistance Liner Concept for High-Pressure Thrust Chamber Applications", Rocketdyne Division of North American Aviation, Research Report No. 64-28, (August 1964).

26. Sellers, J. P., Jr., "Effects of Carbon Deposition on Heat Transfer in a LOX/RP-1 Thrust Chamber", ARS Journal, 31, No. 5, (1961).

27. Dyban, E. P., Shvets, I. T., Air Cooling of Gas Turbine Rotors, Izdatei'stvo Kievskogo Universiteta Kiev, (1959).

28. Kapinos, V. M., Il'chenko, O. T., "Thermal Resistance of Turbine Blade Base Joints", Energomashinostronenie, 5, No. 6, 23-26, (1959).

29. Shvets, I. T., "Study of Contact Heat Exchange Between Heat Engine Parts", Proc. Inst. Power Engr, UKSSR, No. 12, (1955).

30. Gardner, K. A., Carnavos, T. C., "Thermal Contact Resistance in Finned Tubing", J. Heat Transfer, ASME, 82C, 279-293, (1960).

REFERENCES (Cont'd)

31. Atkins, H. L., Fried, E., "Thermal Interface Conductance in a Vacuum", AIAA Paper No. 64-253, (July 1964).

32. Fried, E., "Study of Interface Thermal Contact Conductance", General Electric Company, Summary Report, NASA Contract No. NAS 8-5207, (May 1964).

33. Clausing, A. M., Chao, B. T., "Thermal Contact Resistance in a Vacuum Environment", ASME Paper No. 64-HT-16, (August 1964).

34. Kaspareck, W. E., Dailey, R. M., "Measurements of Thermal Contact Conductance in a Vacuum", NASA Marshall Space Flight Center, Report No. AD 439, 477, (March 1964).

35. Kaspareck, W. E. Dailey, R. M., "Measurements of Thermal-Contact Conductance Between Dissimilar Metals in a Vacuum", ASME Paper No. 64-NT-38, (August 1964).

36. Janşson, R. M., "The Heat Transfer Properties of Structural Elements for Space Instruments", Project Apollo, M.I.T. Instrumentation Laboratory Report No. E-1173, (June 1962).

37. Bloom, M. F., "Thermal Contact Conductance in a Vacuum Environment", Douglas Aircraft Company Report No. SM 47700, (December 1964).

38. Fried, E., Costello, F. A., "Interface Thermal Contact Resistance Problem in Space Vehicles", ARS Journal, 32, 237-243, (February 1962).

39. Fried, E., "Thermal Joint Conductance in a Vacuum", ASME Paper No. AGHT-18, (March 1963).

40. Stubstad, W. R., "Measurements of Thermal Contact Conductance in Vacuum", ASME Paper No. 63-WA-150, (November 1963).

41. Petri, F. J., "An Experimental Investigation of Thermal Contact Resistance in a Vacuum", ASME Paper 63-WA-156, (November 1963).

42. Armand, G., Lapujaulade, J., Paigne, J., "A Theoretical and Experimental Relationship Between the Leakage of Gases Through the Interface of Two Metals In Contact and Their Superficial Micro Geometry", Vacuum, 14, No. 2, 53-57, (1964).

43. Mikesell, R. P., Scott, R. B., "Heat Conduction Through Insulating Supports in Very Low Temperature Equipment", J. Res. NBS, 57, No. 6, 371-378, (1956).

44. Thomas, J. R., Probert, S. D., "Variation of Thermal Conductance of Multi-layer Stacks Under Load", Welch College of Adv Tech., Int'l Conf. on Thermal Conductivity, London, (1964).

45. Berman, R., "Some Experiments on Thermal Contact at Low Temperatures", J. Appl. Phys., 27, No 4, 318-323, (1956).

REFERENCES (Cont'd)

46. Berman, R., Mate, C. F., "Thermal Contact at Low Temperatures", Nature, 182, 1661-63, (1958).

47. Little, W. A., "The Trasnsport of Heat Between Dissimilar Solids at Low Temperatures", Can. J. Phys, 37, 334-49, (1959).

48. Vickers, J. M. F., "A Study of Thermal Scale Modeling Techniques", Jet Propulsion Laboratory Tech Memo No. 33-153, (September 1963).

49. Fowle, A. A., Gabron, F., Johnson, R. W., "Thermal Scale Modeling of Spacecraft: An Experimental Investigation", A. D. Little Co., Inc., Report C-64924, (June 1963).

50. Bevans, J. T., "Prediction of Space Vehicle Thermal Performance", Space Technology Laboratories, Bimonthly Progress Reports 1-3, (August-December 1964).

51. Speeds, J. A., Fuller, L. E., "Feasibility Investigation of a Moving Belt Radiator", Rocketdyne Division of North American Aviation, ASD-TDR-63-551, (August 1963).

52. Ibid, Quarterly Progress Report No. 3, Contract AF 33(615)-1574, (January 1965).

53. Brutto, I., Casagrande, I., Perona, G., "Thermal Contact Resistance Between Cylindrical Metal Surfaces", Energia Nucleare, (Milan), 6, 532-540, (1959).

54. Wheeler, R. G., "Thermal Conductance of Fuel Element Materials", Hanford Atomic Products Operation, AEC Report No. HW 60343, (1959).

55. Boeschoten, F., "On the Possibility to Improve the Heat Transfer of Uranium and Aluminum Surfaces in Contact", Proc. Int'l Conf on Peaceful Uses of Atomic Energy, 9, 208-9, Geneva, (1955).

56. Fenech, H., Rohsenow, W. M., "Prediction of Thermal Conductance of Metallic Surfaces in Contact", J. Heat Transfer, 85, 15-24, (Feb 1963).

57. Ibid, AEC Report No. NYO-2163, (1959).

58. Henry, J. J., Fenech, H., "The Use of Analog Computers for Determining Surface Parameters Required for Prediction of Thermal Contact Conductance", J. Heat Transfer, 86, 543-551, (November 1964).

59. Henry, J. J., "Some Methods of Surface Analysis for the Prediction of Thermal Resistance of Metal Contacts", AEC Report No. NYO-9457, (1961).

60. Ibid, "Thermal Conductance of Metallic Surfaces in Contact", AEC Report No. NYO-9459, (1963).

61. Sanderson, P. D., "Heat Transfer from the Uranium Fuel to the Magnox Can in a Gas-Cooled Reactor", Int'l Dev in Heat Trans, Part I, No. 8, 53-64, (1961).

REFERENCES (Cont'd)

62. Robertson, J. A. L., Ross, A. M., Notley, M. J. F., MacEwan, J. R., "Temperature Distribution in UO_2 Fuel Elements", J. Nuclear Materials, 7, 225-263, (1962).

63. Rapier, A. C., Jones, I. M., McIntosh, J. E., "The Thermal Conductance of UO_2/ Stainless Steel Interfaces", Int. J. Heat Mass Transfer, 6, 397-416, (May 1963).

64. Neider, H., "Thermal Conductance Tests on Hanford Fuel Element Bonds", AEC Report No. HW 33, 741, (March 1955).

65. Skipper, R. G. S., Wooten, K. J. "Thermal Resistance Between Uranium and Can", Proc 2nd Int'l Conf. on Peaceful Uses of At. Energy, 7, 684-690, (1958).

66. Ascoli, A., Germagnoli, E., "Measurement of the Thermal Contact Resistance Between Flat Surfaces of Uranium and Aluminum", Energia Nuclear (Milan), 3, No. 1, 23-31, (Feb 1956).

67. Boeschoten, F., van der Held, E. F. M., "The Thermal Conductance of Contacts Between Aluminum and Other Metals", Physica, 23, 37-44, (1957).

68. Miller, V. S., "Pecularities of Contact Heat Exchange Transfer in Fuel Elements of a Reactor", Izv. Uyssh UCHEB, Zau. Energetika No. 3, 67-70, (1962).

69. Miller, V. S., "Problems Concerning Contact Heat Resistances of Heat Emitting Elements", Zbir. Prats. Inst. Tepl. An. USSR, 24, 133-139, (1962).

70. Shlykov, Yu. P., Ganin, E. A., "Thermal Resistance of Metallic Contacts", Int. J. Heat Mass Trans., 7, No. 8, 921-929, (Aug 1964).

71. Shlykov, Yu. P., Ganin, E. A., "Thermal Contact Resistance", Atomeya Energiya, 9, No. 6, 496-498, (Dec 1960).

72. Holm, R., "Electrical Contacts", Almquist and Wiksells Akademiska Handbooken, Hugo Gebers Forlog, Stockholm, (1958).

73. Holm, R., "Calculation of Temperature Developed in a Contact Heated in the Contact Surface and Application to the Problem of the Temperature Rise in a Sliding Contact", J. Appl. Phys., 15, 361-366, (1948).

74. Holm, R., "Temperature Development in a Heated Contact with Application to Sliding Contacts", J. Appl. Phys. 19, 369-374, (1952).

75. Starr, C., "The Copper Oxide Rectifier", Physics, 7, No. 1, 15-19, (1936).

76. Davis, W., "Thermal Transients in Graphite-Copper Contacts", Brit J. Appl Phys, 10, No. 12, 516-522 (1959).

77. Ward, A. L., "Dependence of Metal-to-Semiconductor Contact Resistance Upon Contact Loading", Diamond Ordnance Laboratories TR-731, (1959).

REFERENCES (Cont'd)

78. Epstein, J. M., "Contact Resistance: Its Measurement and Effect on the Performance of High-Wattage Thermoelectric Couples", Adv Energy Conv, 2, 113, (1962).

79. Mengali, O. J., Seiler, M. R., "Contact Resistance Studies on Thermoelectric Materials", Adv Energy Conv, 2, 59-68, (1962).

80. Cutler, M., "Small Area Contact Methods", Adv Energy Conv, 2, 29-43, (1962).

81. Powell, R. W., "Experiments Using a Simple Thermal Comparator for Measurement of Thermal Conductivity, Surface Roughness and Thickness of Foils or of Surface Films", J. Sci Instr (G.B.), 34, 485-492, (1957).

82. Clark, W. T., Powell, R. W., "Measurement of Thermal Conduction by the Thermal Comparator", J. Sci. Instr. (G.B.), 39, 545-551, (1962).

83. Powell, R.W., Tye, R.P., "The Thermal Comparator in Non-Destructive Testing", Techniques of Non-destructive Testing, 175, Butterworths, London, England, (1960).

84. Powell, R. W., Tye, R. P., Jolliffe, B. W., "Heat Transfer at Interface of Dissimilar Materials, Evidence of Thermal Comparator Experiments", Int. J. Heat Mass Trans, 5, 897-902, (Oct 1962).

85. Kottler, F., "Elektrostatik der Leiter", Handbuch der Physik, Band 12, 472-473 Springer, Berlin (1927).

86. Holm, R., Elektrische Kontakte, 13-17, Springer-Verlag, Berlin (1958).

87. Centinkale, T. N., Fishenden, M., "Thermal Conductance of Metal Surfaces in Contact", General Discussion on Heat Transfer, 271-275, (Sept 1951).

88. Clausing, A. M., Chao, B. T., "Thermal Contact Resistance in a Vacuum Environment", Department of Mechanical and Industrial Engineering, University of Illinois, Report No. ME-TN-242-1, (August 1963).

89. Roess, L. C., "Theory of Spreading Conductance", Appendix A, Unpublished Report, Beacon Laboratories of Texas Company, Beacon, New York.

90. Laming, L. C., "Thermal Conductance of Machined Metal Contacts", Int'l Dev. Heat Transfer - ASME - Proc Int'l Heat Transfer Conf., (1963).

91. Wong, H. Y., "Thermal Conductance of Metallic Contacts - A Survey", International Symposium on Thermal Conductivity, National Physical Laboratory, England, (1964).

92. Timoshenko, S., Goodier, J. N., Theory of Elasticity, McGraw Hill Book Co., New York, New York, (1951).

93. Bowden, F. P., Tabor, D., The Friction and Lubrication of Solids, Oxford, Clarendon Press, London, (1950).

REFERENCES (Cont'd)

94. Tabor, D., The Hardness of Metals, Oxford, Clarendon Press, London, (1951).

95. Grodzinski, P., "Micro-indentation Hardness", Metallurgia, Vol 50, 125, (Sept 1954).

96. Mott, B. W., Microindentation Hardness Testing, Butterworths Scientific Publications, London, (1952).

97. Tachibana, F., "Study on Thermal Resistance of Contact Surfaces", Nihon Kikai Gakulai Shi, 55, No. 397, pp 102-107, (1952).

98. Cordier, H., "Experimental Study of Contact Thermal Resistances", Annales de Physique, No. 1-2, p 5-19, (1961).

99. Cordier, H., Maimi, R., C.R., 250, 2853-2855, (1960).

100. Bory, Ch., Cordier, H., "Thermal Contact Resistances", French Institute for Fuels and Energy, Transmission of Heat Seminar, pp 1-14, (1961).

101. American Standards Association, "Classification and Design of Surface Qualities ASA Standard B-46; Surface Roughness, Waviness and Lay - ASA B-46.1", (1947).

102. Reason, R. E., Measurement of Surface Texture, Cleaver-Hume Press Ltd. London, (1960).

103. Halliday, J. S., "Surface Examination by Reflection Electron Microscopy", Inst. Mech Engr Proc, 169, 777-781, (1955).

104. Dyson, J., Hirst, W., "The True Contact Area Between Solids", Phy Soc London Proc. 67, Sec B, 309-312, (1954).

105. Shvetsova, E. M., "Determination of Actual Surface Contact Areas on Transparent Models", Institut Mashinovedenia Sbornik, 7, 12-33, (1953).

106. Keegan, H. J., Scheter, J. C., Weidner, V. R., "Effects of Surface Texture on Diffuse Spectral Reflectance", Proc Int'l Sym Thermal Radiation in Solids, Vol I, No. 6, (1964).

107. Archard, J. F., "Contact and Rubbing of Flat Surfaces", J. Appl Phys, 24, No. 8, 981-988, (August 1958).

108. Ling, F. F., "On Asperity Distributions of Metallic Surfaces", J. Appl Phys, 29, No. 8, (August 1958).

109. Myers, N. O., "Characteristics of Surface Roughness", Wear, 5, 182-189, (1962).

110. Held, W., "Heat Transfer Between Worked Surfaces", Allgemeine Warmetechnik, 8, No. 1, 1-8, (1957).

111. Shlykov, Yu. P., Ganin, E. A., Demkin, N.B. "Analysis of Contact Heat Exchange" Teplaemergetola, 7, No. 6, 72-76, (1960).

REFERENCES (Cont'd)

112. Shlykov, Yu. P., Ganin, E. A., "Experimental Study of Contact Heat Exchange", Teploeregetika, 7, 73-76, (1961).

113. Dyban, E. P., Shvets, I. T., Kondac, N. M., "Constant Heat Transfer Between Machine Components", Izvestia Akad, Nauk, SSSR, No. 9, 63-79, (1954).

114. Sonokama, K., "Contact Thermal Resistance", J. JSME, 64, No. 502, 240-250, (1961).

115. Keller, J. D., Iron and Steel Engineering, 11, 60, (1948).

116. Kouwenhoven, W. B., Potter, J. H., "Thermal Resistance of Metal Contacts", J. Am Weld Soc, Vol 27, Part 2, 512-520, (1948).

117. Weills, N. D., Ryder, E. A., "Thermal Resistance Measurements of Joints Formed Between Stationary Metal Surfaces", Trans ASME, Vol 71, No. 3, 253-257, (1949).

118. Kennard, E. H., Kinetic Theory of Gases, McGraw Hill Book Co., New York, N.Y., (1933).

119. Ross, A. M., Stoute, R. L., "Heat Transfer Coefficient Between UO_2 and Zircaloy 2", Report CRFD 1075, Atomic Energy of Canada Limited, (1962).

120. Graff, W. J. "Thermal Conductance across Metal Joints", Machine Design, 32, No. 19, 166-172, (1960).

121. Brunot, A. W., Buckland, F. F., "Thermal Contact Resistance of Laminated and Machined Joints", Trans ASME, 71, 253-257, (1949).

122. Jacobs, R. B. Starr, C., Thermal Conductance of Metallic Contacts", Rev Sci Instr, 10, 140-141, (1939).

123. Hsiech, C. K., "On the Nature of Thermal Contact Conductance", M. Sc. Thesis, Mechanical Engineering Department, Purdue University, (1964).

UNCLASSIFIED
Security Classification

DOCUMENT CONTROL DATA - R&D
(Security classification of title, body of abstract and indexing annotation must be entered when the overall report is classified)

1. ORIGINATING ACTIVITY (Corporate author)
Air Force Materials Laboratory
Research & Technology Division
Air Force Systems Command
Wright-Patterson AFB, Ohio 45433

2a. REPORT SECURITY CLASSIFICATION
UNCLASSIFIED

2b. GROUP

3. REPORT TITLE
Thermal Contact Resistance: Volume I - A Review of the Literature

4. DESCRIPTIVE NOTES (Type of report and inclusive dates)
January 1964 to May 1965, First Report of a 3 Volume Series

5. AUTHOR(S) (Last name, first name, initial)
MINGES, MERRILL L.

6. REPORT DATE	7a. TOTAL NO. OF PAGES	7b. NO. OF REFS
April 1966	70	123

8a. CONTRACT OR GRANT NO.	9a. ORIGINATOR'S REPORT NUMBER(S)
b. PROJECT NO. 7381	AFML-TR-65-375
c. Task No. 738106	9b. OTHER REPORT NO(S) (Any other numbers that may be assigned this report)
d.	

10. AVAILABILITY/LIMITATION NOTICES
This document is subject to special export controls and each transmittal to foreign governments or foreign nationals may be only with prior approval of the Materials Engineering Branch of the Air Force Materials Laboratory.

11. SUPPLEMENTARY NOTES	12. SPONSORING MILITARY ACTIVITY
	AFML, RTD, AFSC Wright-Patterson AFB, Ohio

13. ABSTRACT

The objective of this report has been to critically review the status of experimental and analytical developments in the area of heat transfer across interfaces of solids in contact. The nature of the heat flow patterns which develop across an imperfect interface are first discussed along with the equations defining the thermal contact resistance parameter. Following this a general discussion is given of the practical application areas where interface heat transfer is an important design parameter. The next sections of the report give a thorough presentation of the analytical analyses which have been developed to describe this phenomena. Surface deformation effects, geometrical characterization of surfaces and the influences of void phase conduction are outlined. Correlations of experimental results with analytical predictions are covered in the final section using the equations derived for the single and multiple contact cases. Some of these correlations are based on limited experimental data, others are more generalized in nature.

DD FORM 1 JAN 64 1473

UNCLASSIFIED
Security Classification

14. KEY WORDS	LINK A		LINK B		LINK C	
	ROLE	WT	ROLE	WT	ROLE	WT
Interface Heat Transfer Solid-Solid Contacts Thermal Contact Resistance Thermal Conductivity Heat Transfer Coefficients Contacting Surfaces						

INSTRUCTIONS

1. ORIGINATING ACTIVITY: Enter the name and address of the contractor, subcontractor, grantee, Department of Defense activity or other organization *(corporate author)* issuing the report.

2*a*. REPORT SECURITY CLASSIFICATION: Enter the overall security classification of the report. Indicate whether "Restricted Data" is included. Marking is to be in accordance with appropriate security regulations.

2*b*. GROUP: Automatic downgrading is specified in DoD Directive 5200.10 and Armed Forces Industrial Manual. Enter the group number. Also, when applicable, show that optional markings have been used for Group 3 and Group 4 as authorized.

3. REPORT TITLE: Enter the complete report title in all capital letters. Titles in all cases should be unclassified. If a meaningful title cannot be selected without classification, show title classification in all capitals in parenthesis immediately following the title.

4. DESCRIPTIVE NOTES: If appropriate, enter the type of report, e.g., interim, progress, summary, annual, or final. Give the inclusive dates when a specific reporting period is covered.

5. AUTHOR(S): Enter the name(s) of author(s) as shown on or in the report. Enter last name, first name, middle initial. If military, show rank and branch of service. The name of the principal author is an absolute minimum requirement.

6. REPORT DATE: Enter the date of the report as day, month, year; or month, year. If more than one date appears on the report, use date of publication.

7*a*. TOTAL NUMBER OF PAGES: The total page count should follow normal pagination procedures, i.e., enter the number of pages containing information.

7*b*. NUMBER OF REFERENCES: Enter the total number of references cited in the report.

8*a*. CONTRACT OR GRANT NUMBER: If appropriate, enter the applicable number of the contract or grant under which the report was written.

8*b*, 8*c*, & 8*d*. PROJECT NUMBER: Enter the appropriate military department identification, such as project number, subproject number, system numbers, task number, etc.

9*a*. ORIGINATOR'S REPORT NUMBER(S): Enter the official report number by which the document will be identified and controlled by the originating activity. This number must be unique to this report.

9*b*. OTHER REPORT NUMBER(S): If the report has been assigned any other report numbers *(either by the originator or by the sponsor)*, also enter this number(s).

10. AVAILABILITY/LIMITATION NOTICES: Enter any limitations on further dissemination of the report, other than those imposed by security classification, using standard statements such as:

(1) "Qualified requesters may obtain copies of this report from DDC."

(2) "Foreign announcement and dissemination of this report by DDC is not authorized."

(3) "U. S. Government agencies may obtain copies of this report directly from DDC. Other qualified DDC users shall request through _____."

(4) "U. S. military agencies may obtain copies of this report directly from DDC. Other qualified users shall request through _____."

(5) "All distribution of this report is controlled. Qualified DDC users shall request through _____."

If the report has been furnished to the Office of Technical Services, Department of Commerce, for sale to the public, indicate this fact and enter the price, if known.

11. SUPPLEMENTARY NOTES: Use for additional explanatory notes.

12. SPONSORING MILITARY ACTIVITY: Enter the name of the departmental project office or laboratory sponsoring *(paying for)* the research and development. Include address.

13. ABSTRACT: Enter an abstract giving a brief and factual summary of the document indicative of the report, even though it may also appear elsewhere in the body of the technical report. If additional space is required, a continuation sheet shall be attached.

It is highly desirable that the abstract of classified reports be unclassified. Each paragraph of the abstract shall end with an indication of the military security classification of the information in the paragraph, represented as *(TS), (S), (C), or (U)*.

There is no limitation on the length of the abstract. However, the suggested length is from 150 to 225 words.

14. KEY WORDS: Key words are technically meaningful terms or short phrases that characterize a report and may be used as index entries for cataloging the report. Key words must be selected so that no security classification is required. Identifiers, such as equipment model designation, trade name, military project code name, geographic location, may be used as key words but will be followed by an indication of technical context. The assignment of links, rules, and weights is optional.

GPO 886-551